

See discussions, stats, and author profiles for this publication at: <https://www.researchgate.net/publication/23975801>

Simulation of the First Hydration Shell of Nucleosides D4T and Thymidine: Structures Obtained Using MP2 and DFT Methods

ARTICLE *in* THE JOURNAL OF PHYSICAL CHEMISTRY B · MARCH 2009

Impact Factor: 3.3 · DOI: 10.1021/jp806684v · Source: PubMed

CITATIONS

27

READS

45

4 AUTHORS, INCLUDING:



Mauricio Alcolea Palafox

Complutense University of Madrid

129 PUBLICATIONS 1,440 CITATIONS

[SEE PROFILE](#)



Mercedes De la Fuente

National Distance Education University

13 PUBLICATIONS 104 CITATIONS

[SEE PROFILE](#)

Article

Simulation of the First Hydration Shell of Nucleosides D4T and Thymidine: Structures Obtained Using MP2 and DFT Methods

M. Alcolea Palafox, N. Iza, M. de la Fuente, and R. Navarro

J. Phys. Chem. B, 2009, 113 (8), 2458-2476 • DOI: 10.1021/jp806684v • Publication Date (Web): 03 February 2009

Downloaded from <http://pubs.acs.org> on March 18, 2009

More About This Article

Additional resources and features associated with this article are available within the HTML version:

- Supporting Information
- Access to high resolution figures
- Links to articles and content related to this article
- Copyright permission to reproduce figures and/or text from this article

[View the Full Text HTML](#)



ACS Publications

High quality. High impact.

The Journal of Physical Chemistry B is published by the American Chemical Society. 1155 Sixteenth Street N.W., Washington, DC 20036

Simulation of the First Hydration Shell of Nucleosides D4T and Thymidine: Structures Obtained Using MP2 and DFT Methods

M. Alcolea Palafox,*† N. Iza,† M. de la Fuente,*‡ and R. Navarro‡

Departamento de Química-Física I, Facultad de Ciencias Químicas, Universidad Complutense, Ciudad Universitaria, Madrid-28040, Spain, and Departamento de Ciencias y Técnicas Fisicoquímicas, Universidad Nacional de Educación a Distancia (UNED), c/ Senda del Rey s/n, Madrid-28040, Spain

Received: July 28, 2008; Revised Manuscript Received: November 24, 2008

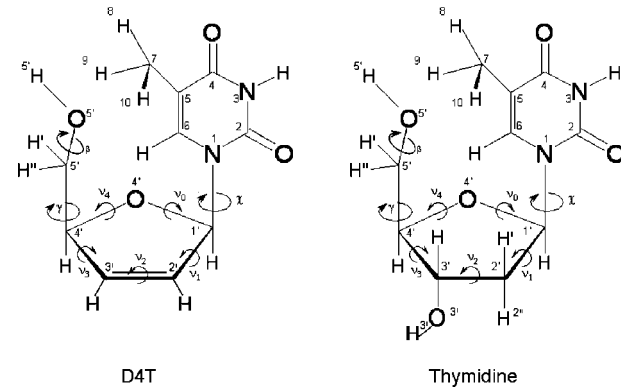
A comparative theoretical analysis on the effect of the solvent on the molecular structure and energetics of the most stable conformers of the nucleoside analogue D4T (stavudine) and of the natural nucleoside thymidine (Thy) was carried out. Solvent effects were considered using the Tomasi's polarized continuum model (PCM) and including a variable number (1–13) of explicit water molecules surrounding the nucleoside in order to simulate the first hydration shell. More than 200 cluster structures with water were analyzed. B3LYP and MP2 quantum chemical methods were used. The CP-corrected interaction energies for D4T and water molecules were computed. For cases where literature data are available, the computed values were in good agreement with previous experimental and theoretical studies. In the isolated state, conformer I (anti-gg-gg) appears the most stable for D4T molecule and conformer II (anti-gg-gt) for Thy molecule. In D4T with eight water molecules, conformer II changes to conformer I. Thus, conformer I seems preferred when water molecules are situated in the first hydration shell. However, in hydrated thymidine conformer Ia (anti-gg-tg) is the more stable one, and the first hydration shell is more extended than in D4T molecule. The effect of the hydration on the total atomic charges and intermolecular distances were also discussed. Several general conclusions on hydrogen bonds network and involved interaction energies were underlined.

1. Introduction

Many different strategies have been developed in the search for therapeutic agents against AIDS. Thus, synthesis of nucleoside analogues,^{1–5} protease inhibitors, integrase inhibitors, and other has been reported.⁶ Actually, nucleoside analogues play a crucial role in the current treatment of cancer and viral infections.^{7–12} D4T (3'-deoxy-2',3'-didehydro-thymidine) is one of the most effective alternative substrates of the HIV-1 reverse transcriptase enzyme. This nucleoside analogue belongs to the NRTIs (nucleoside reverse transcriptase inhibitors), antiviral agents that also have a wide range of other biological activities as antitumor and antibiotic agents. These nucleosides analogues lack a 3'-hydroxyl group, therefore they inhibit further growth of the viral DNA chain. They are the inactive unphosphorylated form (prodrugs), and their activation to the triphosphate form by cellular kinases is required for drug potency. After its phosphorylation to the triphosphate form, they can compete with endogenous nucleotides to inhibit HIV reverse transcriptase,^{1–3,6} and they may also act as a chain terminator by incorporation into growing strands of DNA and RNA. The first phosphorylation is often the rate-limiting reaction in the three-step phosphorylation of several anticancer nucleoside analogues (limits the effectiveness of such drugs). Additionally, a reduction in activity of the deoxyribonucleoside specific cellular kinase is often associated with resistance of cancer cells to these cytotoxic nucleosides.^{13,14}

A number of studies has been carried out aimed at establishing the relationship between structure, conformational features, or

SCHEME 1: Definition of the torsional exocyclic and endocyclic angles in D4T and thymidine molecules



physicochemical properties and activity of these drugs.¹⁵ It has been reported that anti-HIV activity depends upon the ribose conformer.^{16,42b} Differences in the ribose ring puckering lead to appreciable changes in relative positions of the thymine ring and the C5'-OH group. On the other hand, since the nucleosides have several specific sites for forming inter- and intramolecular hydrogen bonds, their conformers are strongly dependent on the solvent characteristics and the experimental conditions.

In the present work, the solvent effect on the geometries and energetics at the highest level of calculation available, under the limitation of the computer memory requirements, has been analyzed. Two different conformers of D4T have been selected for this study: anti-gg-gg (conformer I) and anti-gg-gt (conformer II), related to γ - γ - β angles, Scheme 1. Both conformers have been chosen in base of a complete theoretical conformational analysis of the D4T nucleoside analogues, which has been

* To whom correspondence should be addressed. E-mail: alcolea@quim.ucm.es (M.A.P.), mfuente@ccia.uned.es (M.F.).

† Universidad Complutense.

‡ Universidad Nacional de Educación a Distancia.

performed combining the different orientation around χ - γ - β angles, in steps of 60° ,¹⁷ and taking into account previous conformational features, reported for natural nucleosides and its derivatives.^{47,20b} More details will be specified below (Section 3). Similar studies have been carried out for Thy nucleoside for comparative purposes. To our knowledge, D4T has been extensively examined for antiviral properties, but less structural and energetic information, obtained from theoretical studies, are available. Moreover, they have been calculated at a lower level than that used in this work.^{6,15,18–20a} Analogous studies have been reported with Thy nucleoside.^{20b} The methodology applied to the hydration in the present paper has been previously reported in accurate investigations of the influence of water in the solvation of nucleosides and related molecules,^{20c} and it is detailed in the next section.

2. Calculations

Calculations were carried out using MP2 methods and density functional theory (DFT), including Becke's three-parameter exchange functional (B3) in combination with the correlational functional of Lee, Yang, and Parr (LYP). DFT methods provide adequate compromise between the desired chemical accuracy and the heavy demands put on computer time and power. Moreover, DFT methods have been used satisfactorily in many studies of drug design.^{21a–c} It is well-established that weak interactions are poorly described by DFT methods. However, the hydration of uracil^{21d} and their derivatives has also been studied satisfactory by DFT methods. The interactions due to hydrogen bonding are mainly electrostatic, and they are reasonably well accounted by DFT methods.²²

The B3LYP method was chosen because different studies have shown that the data obtained with this level of theory are in good agreement with those obtained by other more computationally costly methods, such as MP2 calculations, and it predicts vibrational wavenumbers of DNA bases better than the HF and MP2 methods.^{23–28} In all the structures, when computer requirements allowed it, MP2 computations were also performed to confirm or correct the B3LYP results.

The B3LYP and MP2 methods appear implemented in the GAUSSIAN 03 program package.²⁹ Several basis set were used starting from 6–31G* to 6–311++G(3df,pd), but the 6–31G** set represents a compromise between accuracy and computational cost, thus it was the basis set selected for all the calculations. Calculation with Tomasi's polarized continuum model (PCM)^{30,31} was used as implemented in Gaussian 03 by default using the integral equation formalism model, IEF-PCM.³²

The optimum geometry was determined by minimizing the energy with respect to all geometrical parameters without imposing molecular symmetry constraints. Berny optimization under the TIGHT convergence criterion was used. The mean absolute errors for bond lengths reported⁴⁹ by MP2/6–31G** is 0.014 \AA and that by B3LYP/6–311G** is 0.004 \AA . The mean absolute errors in the angles is about 1° by both methods.

Atomic charges were determined with the natural NBO^{33,34} procedure. Because NBO charges appear to be more reliable than the Merz–Kollman and the Mulliken, they were the only ones studied in detail. It should be stressed that the net atomic charges obtained from Mulliken population analysis show extremely strong basis set dependence, and they vary considerably with the method employed in calculations.

The harmonic wavenumber calculations were carried out at the same level of the respective optimization process and by the analytic evaluation of the second derivative of the energy with respect to the nuclear displacement. When it was possible,

the wavenumber calculations were performed in all the optimized conformers to asses that they correspond to real minima. All the optimized structures only showed positive harmonic vibrations (true energy minimum) with exceptions in PCM calculations.

Relative energies were obtained by including zero-point vibrational energies (ZPE). For the calculation of the ZPE, the wavenumbers were retained unscaled.

2.1. Hydration Effects. To theoretically simulate the hydration effects three procedures have been suggested:³⁵ (1) empirical scaling of the quantum mechanical force constants of the isolated molecule³⁶ (2) use of the continuum model³⁷ or (3) modeling of the hydrated compound by including sufficient numbers of explicit water molecules.³⁸

In the discrete methods, water molecules provide a description of both the microscopic structure of the solvent and specific solute–solvent interactions. A selected number of solvent configurations are included in the quantum-mechanical description of the system. Unfortunately, both the large number of solvent molecules required to mimic a dilute solution and the computational cost of quantum-mechanical calculations³⁹ limit the applicability of discrete methods.

The continuum model procedure has a solid theoretical ground, and it is used mostly today, owing mainly to its simplicity and the lower computational time required. However, discrete methods may be preferred since it gives an account of hydrogen bonds explicitly.

In the present paper, calculations with Tomasi's PCM and with an explicit number of water molecules (up to 13) surrounding the nucleoside have been performed. It can be noted that in the simulation with the PCM model, the number of conformers corresponding to real minima is remarkably reduced compared to those found in isolated state.

2.2. Interaction Energies. In the hydration of D4T with explicit water molecules the energies obtained were corrected for basis set superposition error (BSSE) using the counterpoise (CP) procedure from Danilov et al.⁴⁰ The CP-corrected B-(H₂O)_n formation energy for D4T molecule is

$$\Delta E_{\text{BW}_n}^{\text{CP}} = E^{(\text{BW}_n)}(\text{BW}_n) + E^{(\text{def})}(\text{BW}_n) \quad (1)$$

where $B \equiv \text{D4T}$, $W_n \equiv$ water n mer and $E^{(\text{BW}_n)}(\text{BW}_n)$ and $E^{(\text{def})}(\text{BW}_n)$ are defined as:

$$\begin{aligned} E^{(\text{BW}_n)}(\text{BW}_n) &= E_{\text{BW}_n}^{(\text{BW}_n)}(\text{BW}_n) - E_{\text{B}}^{(\text{BW}_n)}(\text{BW}_n) - \\ &\quad E_{\text{W}_1}^{(\text{BW}_n)}(\text{BW}_n) - [...] - E_{\text{W}_n}^{(\text{BW}_n)}(\text{BW}_n) \\ E^{(\text{def})}(\text{BW}_n) &= E_{\text{B}}^{(\text{def})}(\text{BW}_n) + E_{\text{W}_1}^{(\text{def})}(\text{BW}_n) + [...] + \\ &\quad E_{\text{W}_n}^{(\text{def})}(\text{BW}_n) \end{aligned}$$

The deformation energy of monomer X ($X \equiv \text{D4T}$ or W) is:

$$E_{\text{X}}^{(\text{def})}(\text{BW}_n) = E_{\text{X}}^{(\text{X})}(\text{BW}_n) - E_{\text{X}}^{(\text{X})}(X) \quad (2)$$

Here the subscripts denote the molecular system, and the superscripts indicate whether the calculation is done with the basis set of the nucleoside (D4T), the basis set of a water molecule, (W), or the basis set of the entire system, (D4TW_n). The parenthesis indicate whether the calculation is done at the optimized geometry of the entire system, (BW_n), or at the monomer optimized geometry (X).

TABLE 1: Relative Energies (Expressed in AU^a) Calculated for the Different Conformers in Anti-orientation ($\chi \approx -120^\circ$) of D4T Molecule in Isolated State and with the PCM Model, Using Different Levels of Theory

angle γ	B3LYP/6–31G**			B3LYP/6–31G** (PCM)			B971/6–31G**			MP2/6–31G**		
	~60	~−60	~180	~60	~−60	~180	~60	~−60	~180	~60	~−60	~180
$\beta \approx 60$	0.0 ^{b,c}	0.00547	0.00665	0.00144 ^{f,c}	0.00305 ^f	0.00266 ^f	0.0 ^{c,f}	0.00621	0.00768	0.0 ^{c,g}	0.00773	0.00956
$\beta \approx -60$	0.00125 ^h	0.00406	0.00186	0.0 ^{e,h}	0.00252 ^f	0.00166 ^f	0.00138 ^h	0.00484	0.00225	0.00245 ^h	0.00603	0.00343
$\beta \approx 180$	0.00154 ^d	0.00425	0.00679	0.00075 ^d	0.00349	0.00331 ^f	0.00227 ^d	0.00517	0.00799	0.00256 ^d	0.00605	0.00953

^a AU = 627.5095 Kcal/mol. ^b −798.48805 AU. ^c Conformer I. ^d Conformer II, ^e −798.520 95 AU. ^f −798.489 83 AU. ^g −796.427 25 AU. ^h Conformer Ia. ⁱ Saddle points.

The CP corrected interaction energy between the nucleoside ($B \equiv D4T$) and the water n mer (W_n) is calculated according to:

$$\Delta E_{B-(W_n)}^{\text{CP}} = E_{BW_n}^{(BW_n)}(BW_n) - E_B^{(BW_n)}(BW_n) - E_{(W_n)}^{(BW_n)}(BW_n) + E_B^{\text{(def)}}(BW_n) \quad (3)$$

The difference between eqs 1 and 3 is simply the counterpoise-corrected formation energy of a water n mer (in the presence of D4T) at the geometry it adopts in the BW_n complex.

The water–water interaction energy is:

$$\Delta E_{W_n}^{\text{CP}} = E_{(W_n)}^{(BW_n)}(BW_n) - E_{W_1}^{(BW_n)}(BW_n) - [...] - E_{W_n}^{(BW_n)}(BW_n) + E_{W_1}^{\text{(def)}}(BW_n) + [...] + E_{W_n}^{\text{(def)}}(BW_n) \quad (4)$$

3. Results and Discussion

The nucleosides under study, D4T and Thy, were first analyzed in an isolated state (Tables 1–3). The results were compared to those obtained under the hydration process (Tables 2–6).

3.1. D4T in an Isolated State. An important structural characteristic of D4T is the presence of a double bond in the furanose ring, a feature that renders it nearly planar and imparts a high degree of rigidity to furanose. Nevertheless, there are many conformer possibilities depending on the endocyclic and exocyclic torsional angles of the nucleoside. The most important angles, as well as the labeling of the atoms, are defined in Scheme 1.

Two orientations of the base relative to the furanose ring are determined by the value of the glycosylic torsional angle, χ (O4'–C1'–N1–C2) named anti or syn conformations. The exocyclic torsional angle γ (C3'–C4'–C5'–O5') describes the orientation of the 5'-hydroxyl group relative to the furanose ring. The exocyclic torsion angle β (C4'–C5'–O5'–H5') describes the orientation of the hydroxyl hydrogen H5' relative to the furanose ring.

3.1.1. Conformers and Energetics. X-ray studies^{41,42} of these nucleosides have shown that the glycosylic torsion angle is in anti orientation, with this geometry stabilized by the formation of self-associated species. It is also known that there exists a preference for the anti conformer for biological activity.⁴³

Our previous works, analyzing the potential energy surface (PES) of D4T with 5832 points, establishes that the most stable conformers have χ values around -120° .¹⁷ Thus, for the present work and without any restriction, the optimized geometries of 9 conformers, with $\chi \approx -120^\circ$ and β and γ around 60, −60, and 180° , were analyzed by browsing in this way all possible orientations. Their relative calculated energies appear collected in Table 1 at the B3LYP, B971, and MP2 levels. Following

the MP2 energy criterion, the most stable conformer is denoted as conformer I, and the third-most stable, with $\beta = 180^\circ$, is conformer II. Conformer II is in accord to the experimental conformer found in crystals of mono-, oligo-, and polynucleotides,⁴⁷ where the β value is largely limited to the gt range with few deviations. The second lower relative energy corresponds to conformer Ia with $\beta \approx -60^\circ$, which can be considered a mirror image of conformer I, with $\beta \approx 60^\circ$, thus this conformer is not discussed.

Conformer I. In general, the conformers differ very little in energy, corresponding the global minimum to the anti-gg-gg form with respect to χ , γ , and β torsional angles, respectively. This conformer is denoted as I, and it has been plotted in Figure 1. At the B3LYP/6–31G** level the calculated values corresponding to χ , β , and γ in conformer I were -107.6 , 64.9 , and 62.3° (Table 2), respectively. These data are close to those of some of the conformers found experimentally in D4T crystals (conformer “a” in the monoclinic crystals, $\chi = -118.0^\circ$ and $\gamma = 60.6^\circ$). Different values for the χ angle in X-ray structures^{44–46} could be indicating that they are stabilized by the crystal forces. Selected optimum bond lengths and angles of conformer I at the B3LYP and MP2 levels are included in Figure 1, where the proximity of the data with both methods can be observed.

Conformer II. The second conformer considered corresponds to the anti-gg-gt form, is denoted as II, and is shown later in Figure 4. It has the values of $\chi = -123.3^\circ$, $\beta = 164.4^\circ$ and $\gamma = 45.5^\circ$, indicating that γ values around 45 – 65° lead to the most stable forms (Table 3).

The difference of energy between the two conformers is very small, 0.966 kcal/mol at the B3LYP level. This difference increases with the B971 method (1.42 kcal/mol) and the MP2 method (1.61 kcal/mol), Table 1.

A comparison of the most important conformational parameters of these two conformers is shown in Tables 2 and 3. For simplicity, the small endocyclic ribose angles are not included in these tables. The higher endocyclic angles correspond to ν_0 and ν_4 , and all of them are lower than 8° . It is noted that with the 6–31G** basis set, the dipole moment is overestimated by MP2 (5.91 D) and slightly underestimated by the B3LYP method (4.89 D) as compared with that calculated at the B3LYP/6–311++G(3df,pd) level (5.20 D).

3.1.2. Thymine Moiety. Comparing the pyrimidine ring in D4T with the thymine molecule,⁴⁸ it is noted that the ring is also planar, in agreement with the calculated and experimental results, and the bond lengths and angles do not differ significantly. The lengths of the C–N and C–C single bonds are intermediate between those of the corresponding aromatic and the saturated bonds. Hence, there is some aromatic character on the ring structure. The C4=O4 bond length is apparently a little longer than the C2=O2 bond due to the weak interaction between O4 and the hydrogens of the methyl group. Torsional angles of the thymine ring are in general lower than 2° , in

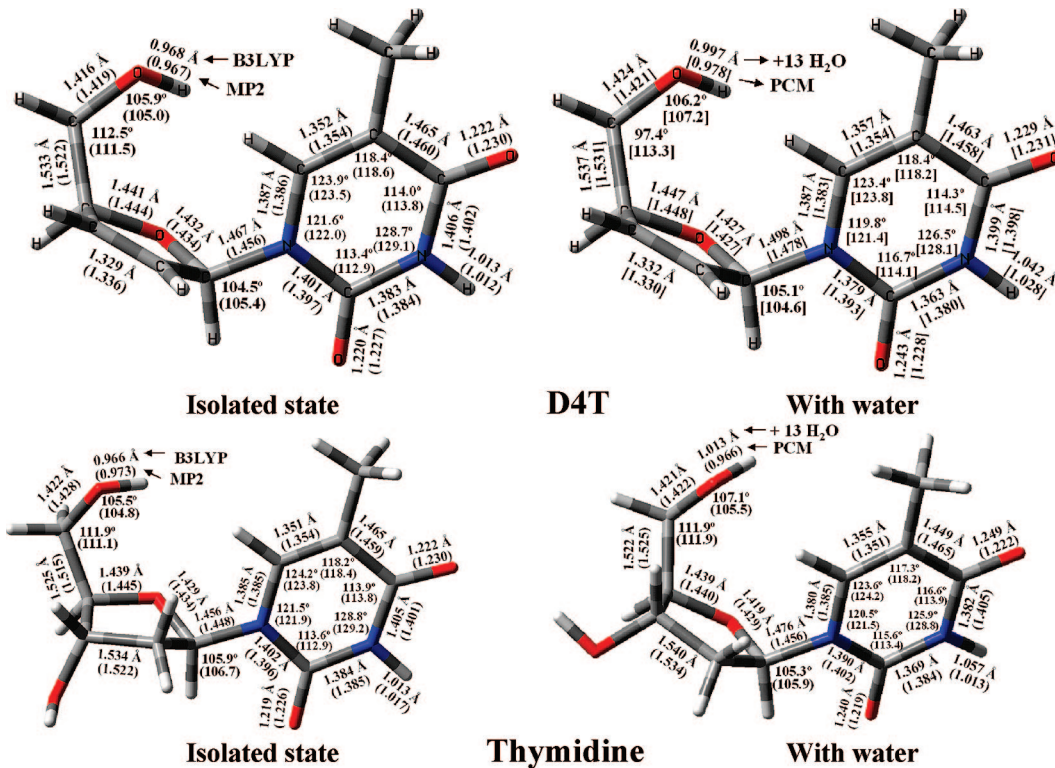


Figure 1. Optimized bond lengths and angles in isolated state of conformer I of D4T and Thy at the B3LYP/6-31G** and MP2/6-31G** (in parentheses) levels.

TABLE 2: Optimum Parameters, Torsional Angles (in degrees), and Dipole Moment (in Debye) Calculated in the Global Minimum of Conformer I in D4T at the B3LYP/6-31G level (in Parentheses at the MP2/6-31G*)**

D4T conformer I	χ	β	γ	pseudo rot. angle phase P^a	dipole moment
D4T isolated	-107.6 (-103.4)	64.9 (63.9)	62.3 (60.5)	80.68 (77.16)	4.89 (5.91)
PCM	-104.3	84.7	59.3	79.13	6.56
1 H ₂ O	-114.9 (-111.9)	88.7 (90.9)	59.9 (55.7)	76.86 (74.45)	3.95 (4.98)
2 H ₂ O	-104.1 (-105.9)	92.3 (92.7)	57.8 (54.9)	69.48 (73.94)	3.03 (2.74)
3 H ₂ O	-104.9 (-106.8)	92.5 (92.3)	57.8 (55.0)	44.27 (72.2)	4.18 (4.10)
4 H ₂ O	-90.7 (-100.8)	96.4 (93.6)	55.3 (54.1)	-57.73 (66.08)	1.97 (1.84)
5 H ₂ O	-89.3	97.5	56.1	-74.59	2.52
6 H ₂ O	-89.4	97.8	55.4	-85.09	5.09
7 H ₂ O	-89.0	92.9	56.4	87.51	2.00
8 H ₂ O	-86.7	92.0	56.7	-89.27	3.29
9 H ₂ O	-78.8	87.8	63.5	-81.17	5.10
10 H ₂ O	-77.7	82.1	63.2	-69.61	6.31
11 H ₂ O	-74.6	63.0	71.9	-66.14	7.23
12 H ₂ O	-68.8	77.3	69.5	-63.94	6.15
13 H ₂ O	-72.0	77.5	65.6	-67.46	5.26

$$^a \text{tg}P = ((\nu_4 + \nu_1) - (\nu_3 + \nu_0)) / (2\nu_2(\sin(36) + \sin(72)))$$

accordance with previous results on the almost planar uracil²⁷ and pyrimidine⁴⁸ ring.

As in the thymine molecule,⁴⁸ in D4T two conformations were obtained by rotation of the methyl group. Wavenumber calculations of these forms reveal that one of them is a first-order saddle point, whereas another one represents the global minimum of the structure, Figure 1. The difference in energy between both forms is very small, less than 5 cal/mol, thus only the global minimum conformation is discussed in the present manuscript. As compared with the conformation labeled as 2 in thymine molecule (global minimum),⁴⁸ the methyl group in D4T appears very little rotated with a C4-C5-C7-H10 torsional angle of 179.0°, and the values of the bond lengths and angles are the same as that in the thymine molecule. These features indicate

that the furanose moiety does not influence the parameters on the methyl group.

The bulkiness of the substitution in position 1 deforms all the neighbor angles. Thus, the ipso angle C2-N1-C6 is remarkably closed, whereas the N1-C2-N3 and N1-C6-C5 angles are opened ca. 1°.

3.1.3. Furanose Moiety. This moiety consists in an unsaturated ribose ring. In position 1 it appears rotated in anti form with respect to the planar thymine ring, with a calculated χ angle in conformer I of -107.6°. The furanose ring appears as almost planar with a ν_2 torsional angle by B3LYP of approximately 1.2°, and ν_3 of -5.4°. Due to the sp^3 hybridization of the C4' atom, the H₂C5'-O5'-H substituent appears out-of-planar with a C2'-C3'-C4'-C5' torsional angle of -125.4°.

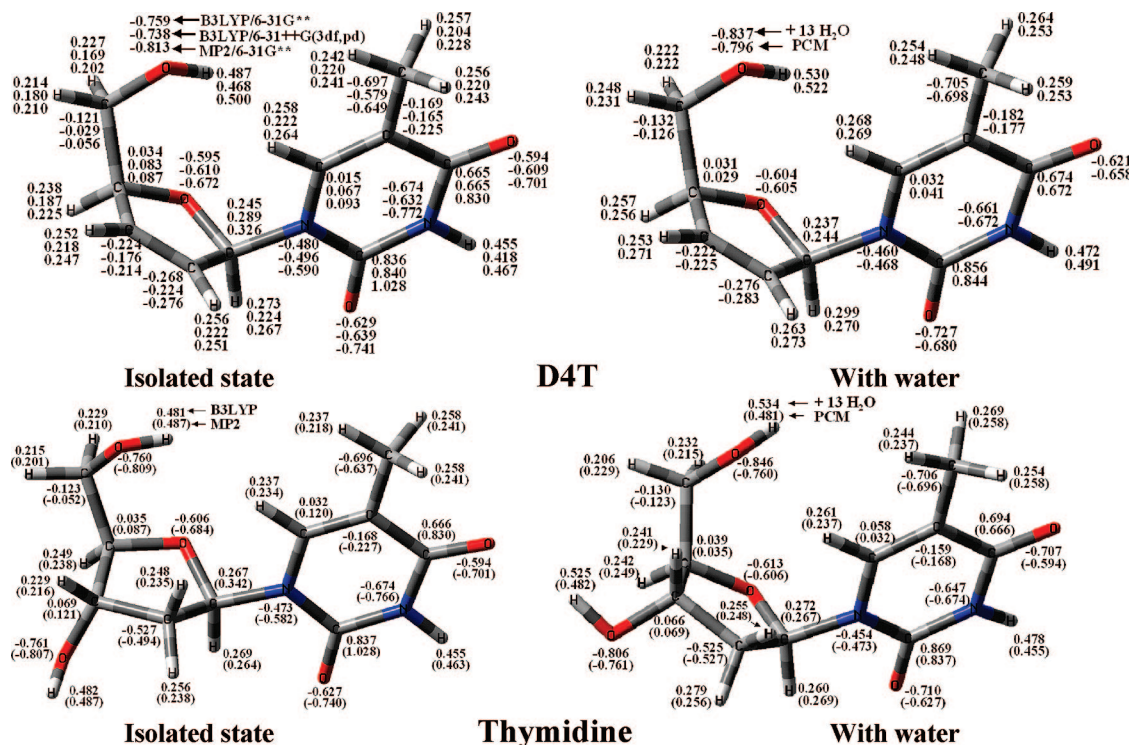


Figure 2. Optimized Natural atomic charges (NBO) of conformer I of D4T and Thy at the B3LYP/6–31G** and MP2/6–31G** (in parentheses) levels.

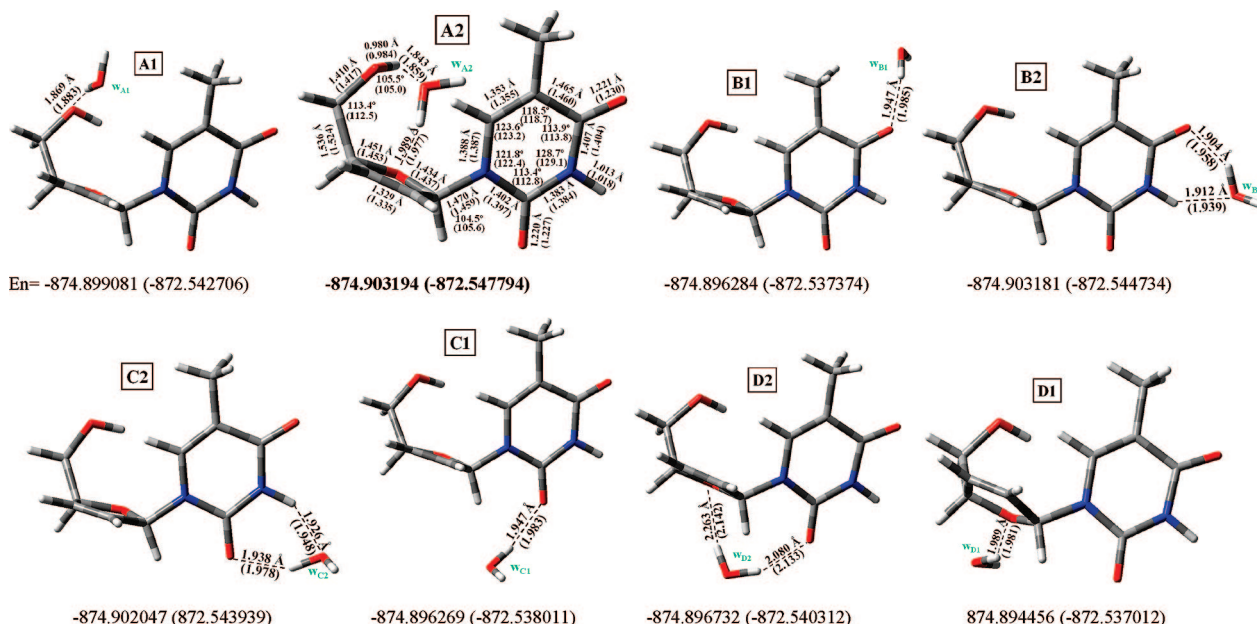


Figure 3. Optimum stable positions of one water molecule in the hydration of conformer I in D4T. The calculated intermolecular H-bonds correspond to B3LYP/6–31G** and MP2/6–31G* (in parentheses) levels. In the bottom of each cluster appears the total energy + ZPE corresponding to B3LYP/6–31G**, and in parentheses the value at the MP2/6–31G* level. For simplicity, weak H-bonds are not shown. The monohydrated cluster with minimum energy is shown in bold type.

The β torsional angle, defining rotation about the C5'-O5' bond, is also of particular interest since, as it is known, the phosphorylation of this group is required to carry out its biochemical activity. In conformer II the calculated value of β by B3LYP was 164.4°. The difference to 180° is due to a slight rotation of hydroxyl group O5'-H by the intramolecular H-bond O5'...H6.

In a general comparison of the results of Figure 1 by B3LYP and MP2 methods, it is noted that MP2 computes the C=O and C2'=C3'' bond lengths slightly longer, and the C4'-C5',

N1-C1', and C4-C5 are slightly shorter. An opening of the C6-N1-C2, C2-N3-C4, and N1-C1'-H1' angles and closing of the N1-C2-N3, C5=C6-N1, C4'-C5'-O5' and C5'-O5'-H5' angles was also observed.

3.1.4. Intramolecular H-Bonds. Although several methods have been suggested for the identification of the H-bonds,^{50a} in the present work we have considered the criterion according to Desiraju et al.^{50b,c} because of the high level of our calculations.

(i) Very strong hydrogen bonds: $1.2 \text{ \AA} < d[\text{H}\cdots\text{A}] < 1.5 \text{ \AA}$, $175^\circ < \text{angle } [\text{X}-\text{H}\cdots\text{A}] < 180^\circ$.

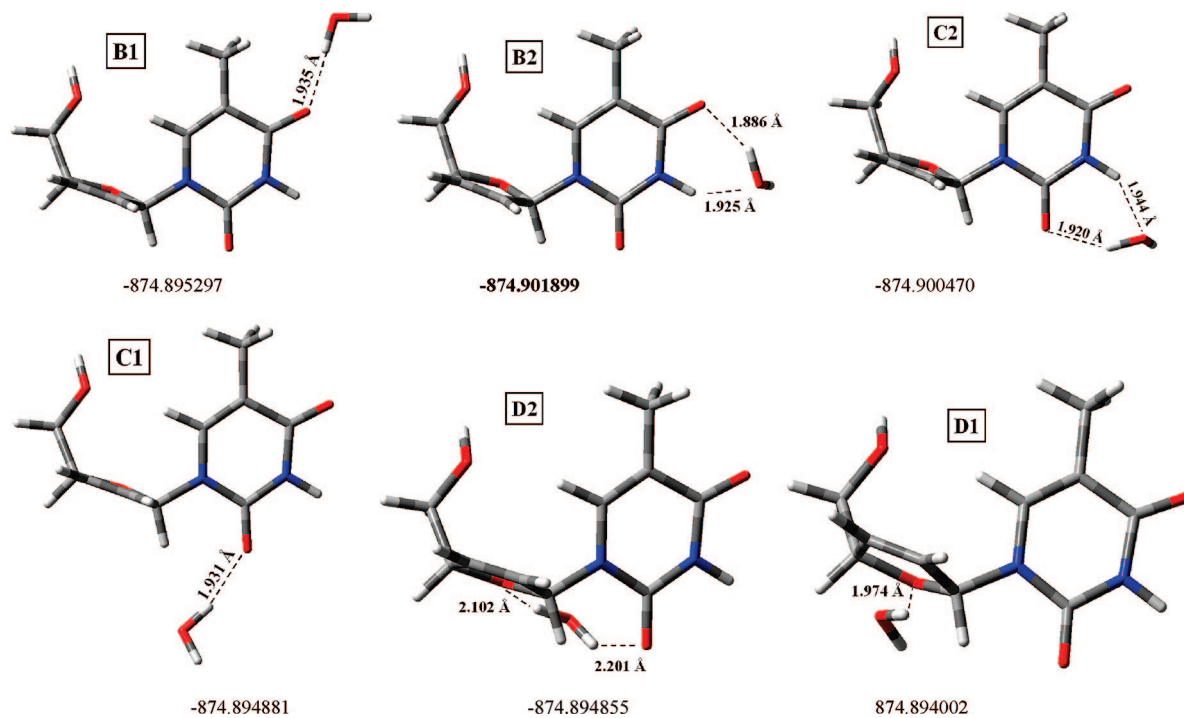


Figure 4. Optimum positions of one water molecule in the hydration of conformer II in D4T at the B3LYP/6-31G** level.

TABLE 3: Optimum Parameters, Torsional Angles (in degrees), and Dipole Moment (in Debye) Calculated in the Global Minimum of Conformer II in D4T at the B3LYP/6-31G Level**

D4T conformer II	χ	β	γ	pseudo rot. angle phase P	dipole moment
D4T isolated	-123.3	164.4	45.5	85.20	6.66
PCM	-124.4	164.3	45.7	89.88	8.62
1 H ₂ O	-124.2	165.7	45.7	85.22	7.31
2 H ₂ O	-124.8	165.2	45.7	85.18	6.56
3 H ₂ O	-124.8	165.6	45.6	85.34	8.29
4 H ₂ O	-142.6	172.2	48.7	79.05	6.50
5 H ₂ O	-140.4	148.5	47.8	73.40	6.48
6 H ₂ O	-141.1	148.1	47.9	72.75	5.47
7 H ₂ O	-137.0	149.8	46.6	78.27	5.36
8 H ₂ O ^a	-111.2	101.7	51.6	66.11	5.13

^a With 9 H₂O molecules, conformer II changes to conformer I; see Table 2.

(ii) Strong hydrogen bonds: $1.5 \text{ \AA} < d[\text{H}\cdots\text{A}] < 2.2 \text{ \AA}$, $130^\circ < \text{angle } [\text{X}-\text{H}\cdots\text{A}] < 180^\circ$.

(iii) Weak hydrogen bonds: $2.0 \text{ \AA} < d[\text{H}\cdots\text{A}] < 3.0 \text{ \AA}$, $90^\circ < \text{angle } [\text{X}-\text{H}\cdots\text{A}] < 180^\circ$.

In D4T, four intramolecular H-bonds can be established in the molecule. In conformer I the values of the intramolecular H-bonds are the following: O₂···H_{1'} is 2.224 Å (2.251 Å by MP2, and 2.239 Å by B3LYP/6-311++G(3df,pd)) and the C_{1'}—H_{1'}···O₂ angle is 109.2° (107.7° by MP2), confirming a weak H-bond between O₂ and H_{1'} atoms. The second possible intramolecular H-bond appears between O_{4'} and H₆. The value of O_{4'}···H₆ is 2.876 Å (2.869 Å by MP2), and the O_{4'}···C₆—H₆ angle is 86.8° (85.4° by MP2), so in this case intramolecular H-bonding does not appear, in contradiction to that reported by Yekeler.¹⁵ The third possible intramolecular H-bond appears between O_{5'} and H₆. The value of O_{5'}···H₆ is 2.511 Å (2.452 Å by MP2, and 2.704 Å by B3LYP/6-311++G(3df,pd)), and the C₆—H₆···O_{5'} angle is 130.7° (126.3° by MP2), confirming a weak H-bond. The fourth possible intramolecular H-bond appears between O_{4'} and H_{5'}. The value of O_{4'}···H_{5'} is 2.700 Å (2.408 Å by MP2 and 2.612 Å by B3LYP/6-311++G(3df,pd)), and the O_{4'}···H_{5'}—O_{5'} angle is 101.3°

(103.2° by MP2 and 96.4° by B3LYP/6-311++G(3df,pd)). So this H-bond is very weak.

Calculations performed at the MP2/6-31G** level in this global minimum,¹⁷ conformer I, confirm these features observed by B97I/6-31G**, B3LYP/6-31G**, and B3LYP/6-311++G(3df,pd). So, in view of these results, intramolecular H-bonding does not appear between O_{4'} and H₆ as reported by Yekeler.¹⁵

In conformer II, the analysis of the three possible intramolecular H-bonds is as follows: the value of O₂···H_{1'} is 2.219 Å (2.245 Å by MP2), and the angle of C_{1'}—H_{1'}···O₂ is 109.7° (108.8° by MP2), confirming a weak H-bond. In the second H-bond the value of O_{4'}···H₆ is 2.629 Å (2.581 Å by MP2), and the angle of C₆—H₆···O_{4'} is 92.8° (93.0° by MP2), so this intramolecular H-bond does not appear, as in conformer I. Finally, the O_{5'}···H₆ is 2.247 Å (2.197 Å by MP2) and C₆—H₆···O_{5'} is 165.1° (165.6° by MP2), so a weak third H-bond is formed.>

3.1.5. Charges. The natural NBO atomic charges on the atoms appear collected in Figure 2 at the B3LYP/6-31G**, B3LYP/6-311++G(3df,pd), and MP2/6-31G** levels. It must

TABLE 4: Optimum Parameters Calculated in the Different Monohydration Forms of Conformer I in D4T at the B3LYP/6-31G** and MP2/6-31G* Levels, Torsional Angles (in Degrees) and dipole moment (in Debye)

cluster	method	χ	β	γ	pseudo rot. angle phase P^a	dipole moment
A1	B3LYP	-97.6	50.9	64.9	80.66	5.25
	MP2	-92.0	51.5	61.9	75.76	6.00
A2	B3LYP	-114.9	88.7	59.9	76.86	3.95
	MP2	-111.9	90.9	55.7	74.45	4.98
B1	B3LYP	-109.0	67.4	62.1	80	5.72
	MP2	-104.5	66.0	60.1	77.06	6.41
B2	B3LYP	-108.7	64.7	62.9	79.78	5.30
	MP2	-104.0	64.1	60.8	76.44	6.21
C2	B3LYP	-107.4	64.8	62.2	80.68	5.85
	MP2	-103.1	63.8	60.2	77.78	6.87
C1	B3LYP	-106.9	65.4	62.4	84.85	3.94
	MP2	-102.2	63.6	60.5	81.66	4.64
D2	B3LYP	-98.7	65.0	60.7	86.37	4.75
	MP2	-94.7	64.7	58.9	82.79	5.68
D1	B3LYP	-106.9	72.2	58.7	79.22	3.23
	MP2	-101.1	69.0	58.0	76.9	3.95

$$^a \text{tg}P = ((\nu_4 + \nu_1) - (\nu_3 + \nu_0))/(2\nu_2(\sin(36) + \sin(72)))$$

TABLE 5: Optimum Parameters Calculated in the Different Monohydration Forms of Conformer II in D4T at the B3LYP/6-31G** Level, Torsional Angles (in Degrees) and Dipole Moment (in Debye)

cluster	χ	β	γ	pseudo rot. angle phase P	dipole moment
B1	-124.6	165.4	45.7	86.46	6.99
B2	-124.2	165.7	45.7	85.22	7.31
C2	-123.2	164.6	45.3	86.04	7.70
C1	-124.4	165.5	45.8	89.27	6.00
D2	-105.4	155.6	45.6	-86.13	7.49
D1	-122.2	162.3	45.4	87.16	5.09

be pointed out that the largest negative charge is on O5' and O2 atoms, with O4 and O4' atoms having similar charge.

Comparing the three levels of theory used it can be noted that MP2 predicts, in most cases, a larger negative charge on the atoms than B3LYP. Also, B3LYP/6-31G** predicts, in general, a larger negative charge on the atoms than B3LYP/6-311++G(3df,pd).

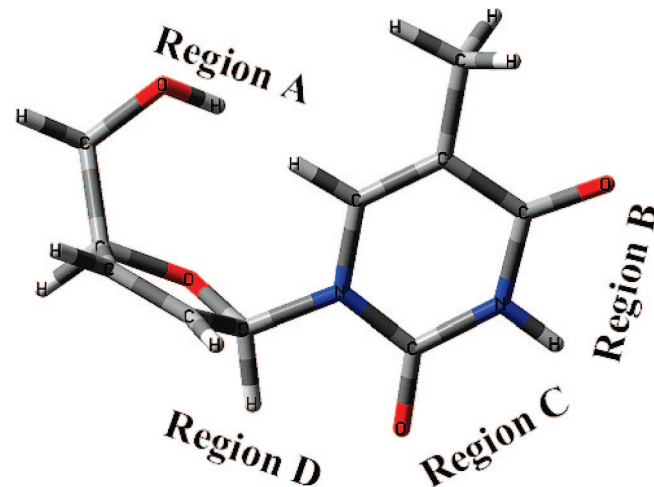
N3 has a negative charge, ca. 0.2 e⁻ (where e⁻ is the charge of an electron), larger than the N1 atom. H5' is the hydrogen atom (hydroxyl group) with highest positive charge, that is, the most reactive one. Closely, the H3 hydrogen charge is only 0.03–0.05 e⁻ lower than H5'. The remaining hydrogen atoms have much less positive charge, in the range 0.17–0.27 e⁻, that is, they are much less reactive.

The highest positive charge corresponds to C2 and C4 atoms, in concordance to the high negative charge on the O2 and O4 atoms, respectively. The O2 oxygen has higher negative charge than O4, so C2 has higher positive charge than C4.

3.2. Thymidine in Isolated State. 3.2.1. Conformers and Energetic. Scheme 1 defines the most important exocyclic and endocyclic torsional angles of the Thy molecule, and Figure 1 plots the global minimum structure optimized at the B3LYP/6-31G** and MP2/6-31G* levels, together with some selected optimized bond lengths and angles. Thymidine appears to have more stable conformers than D4T because of the higher number of degrees of freedom of the system. In contrast to D4T, Thy conformer II is always more stable than conformer I, Table 7. Thus, we discuss the results of both conformers.

Due to the C2'-C3' single bond, the furanose ring is significantly puckered. This ring is twisted out-of-plane in order to minimize nonbonding interactions between their substituents.

3.2.2. Intramolecular H-Bonds. The O2...H1' bond in conformer I of Thy remains similar to D4T, with a value of

SCHEME 2: The four regions in D4T of H-bond formation with water molecules

2.238 Å (2.254 Å by MP2) and C1'-H1'...O2 of 108.4° (107.6° by MP2). The O4'...H6 is very weak or almost null, 2.655 Å (2.636 Å by MP2), and O4'...H6-C6 is 90.4° (89.9° by MP2), as well as the O5'...H6, where the distance is much longer than in D4T (2.980 Å; 2.837 Å by MP2) and O5'...H6-C6 of 149.1° (150.4° by MP2). These facts indicate that the structure consists of weaker H-bonds and that it is more open than in D4T.

Due to the O3'-H3' hydroxyl group of the Thy molecule, two new possible intramolecular H-bonds could appear. However, although the values of the H4'...O3' and H2''...O3' are short, 2.308 and 2.620 Å (2.305 Å and 2.625 Å by MP2), respectively, the angles are too close: C4'-H4'...O3' is 80.3° (79.4° by MP2)

TABLE 6: The CP-Corrected Complex Formation Energy, Interaction Energy, and Deformation Energy between D4T and the Water Molecule (in kcal/mol), Calculated at the B3LYP/6-31G** and MP2/6-31G* Levels in All the Monohydration Clusters with D4T

cluster	conformer I			MP2			conformer II		
	B3LYP			MP2			B3LYP		
	$\Delta E_{\text{D}4\text{T}W1}^{\text{CP}}$ ^a	$\Delta E_{\text{D}4\text{T}-(\text{W}1)}^{\text{CP}}$ ^b	$\Delta E_{\text{D}4\text{T}W1}^{\text{def}}$ ^c	$\Delta E_{\text{D}4\text{T}W1}^{\text{CP}}$ ^a	$\Delta E_{\text{D}4\text{T}-(\text{W}1)}^{\text{CP}}$ ^b	$\Delta E_{\text{D}4\text{T}W1}^{\text{def}}$ ^c	$\Delta E_{\text{D}4\text{T}W1}^{\text{CP}}$ ^a	$\Delta E_{\text{D}4\text{T}-(\text{W}1)}^{\text{CP}}$ ^b	$\Delta E_{\text{D}4\text{T}W1}^{\text{def}}$ ^c
A1	-10.23	-10.32	1.01	-11.51	-11.55	0.94			
A2	-13.32	-13.39	1.03	-14.70	-14.73	1.24			
B1	-8.21	-8.26	0.26	-8.17	-8.15	0.18	-6.51	-6.56	2.35
B2	-13.09	-13.23	0.53	-12.78	-12.84	0.38	-11.08	-11.23	2.60
C2	-12.24	-12.34	0.49	-12.29	-12.32	0.37	-10.14	-10.25	2.56
C1	-8.16	-8.20	0.37	-8.57	-8.55	0.28	-6.11	-6.15	2.45
D2	-8.84	-8.87	0.44	-10.01	-10.01	0.33	-5.35	-5.36	2.71
D1	-6.84	-6.87	0.21	-7.94	-7.93	0.17	-5.53	-5.56	2.21

^a CP-Corrected Complex Formation Energy. ^b Interaction Energy. ^c Deformation Energy.

TABLE 7: Energies (in AU) Calculated in the Two Most Stable Conformers of D4T and Thy Nucleosides

level of theory	D4T		Thy	
	conformer I	conformer II	conformer I	conformer II
Isolated State				
B3LYP/6-31G** (+ZPE)	-798.48805	-798.48651	-874.903915	-874.905374
B3LYP/6-311++G(3df,pd)	-798.98099	-798.98012	-875.458056	-875.458447
MP2/6-31G**	-796.42725	-796.42469	-872.671789	-872.673866
Hydrated Form (PCM)				
B3LYP/6-31G** (+ZPE)	-798.51951 ^c	-798.52020	-874.903912	-874.946535
With 13 H ₂ O Molecules				
B3LYP/6-31G** (+ZPE)	-1791.890305	^a	-1868.319517	-1868.305044 ^b

^a Conformer II changes to conformer I. ^b Conformer Ia. ^c Saddle point.

and C2'—H2''···O3' is 69.7° (68.4° by MP2). These features reveal that intramolecular H-bonds do not appear with the O3'—H3' group.

Similar features were found in conformer II of Thy, with O2'···H1' bond by MP2 of 2.274 Å and C1'—H1'···O2 of 106.6°. The O4'···H6 is also very weak, 2.479 Å, and the O4'···H6—C6 angle too is closed, 94.4°.

3.2.3. Charges. Thy has similar charges to D4T, Figure 2. The main difference is a remarkable increase in the negative charge on the C2' atom, from -0.276 e⁻ by MP2 in D4T to -0.494 e⁻ in Thy. This increase could be explained by the presence of two C2'—H bonds, instead of the double bond in D4T. The C2' atom withdraws negative charge on the neighbor C3' atom, changing from -0.214 e⁻ in D4T to 0.121 e⁻ in Thy, and on C1' atom, changing from 0.326 e⁻ in D4T to 0.342 e⁻ in Thy. Both hydroxyl groups from the Thy molecule show the same charge.

3.3. Hydration. Hydration of DNA takes place through both hydrophilic and hydrophobic sites to form two hydration shells, clearly described in the bibliography. It has been established for some time that there is a shell of tightly bound water molecules at the surface of DNA with significantly different properties from those of bulk water.^{51,52} Experimental results in gas phase reported⁵³ in uracils and thymines reveal an important function of water in protecting our genetic code from photodamage.

A consistent number of studies have focused on the micro-hydration of uracil, which is the structurally simplest base,¹³ and thymine.⁵⁴ It has recently reported that thymine and other nucleobases show that cluster-hydrated structures are energetically preferred over structures with water distributed around the base.^{62b,c} In the present work we studied the cluster-hydrated structures of D4T and Thy nucleosides for the first time.

From early X-ray and neutron diffraction,⁵⁵ it has been well-known that water molecules form hydrogen bonds to the anionic

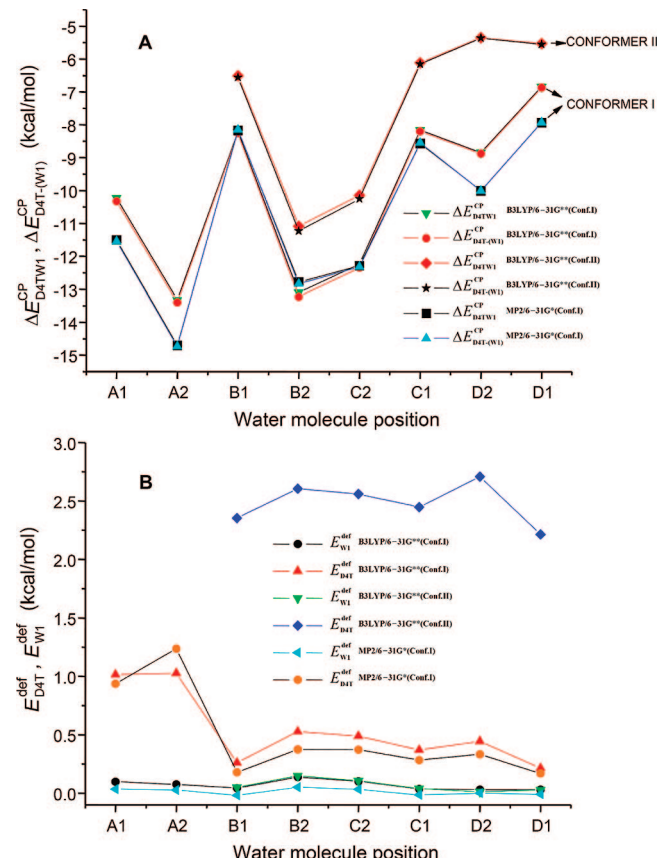


Figure 5. The first water molecule at eight different positions. (A) Complex formation energy and interaction energy between D4T and the water molecule. (B) Deformation energy of the complex and water molecule.

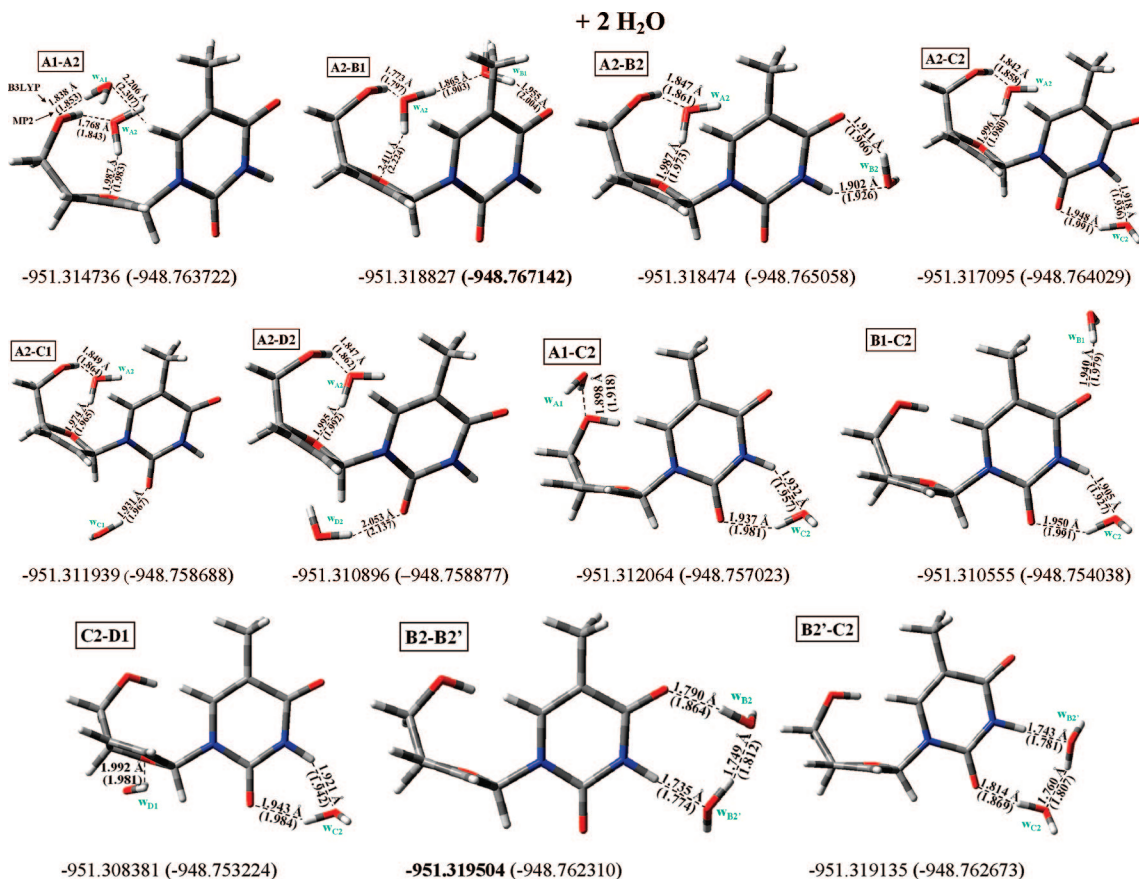


Figure 6. Optimum positions with two water molecules in the hydration of conformer I in D4T.

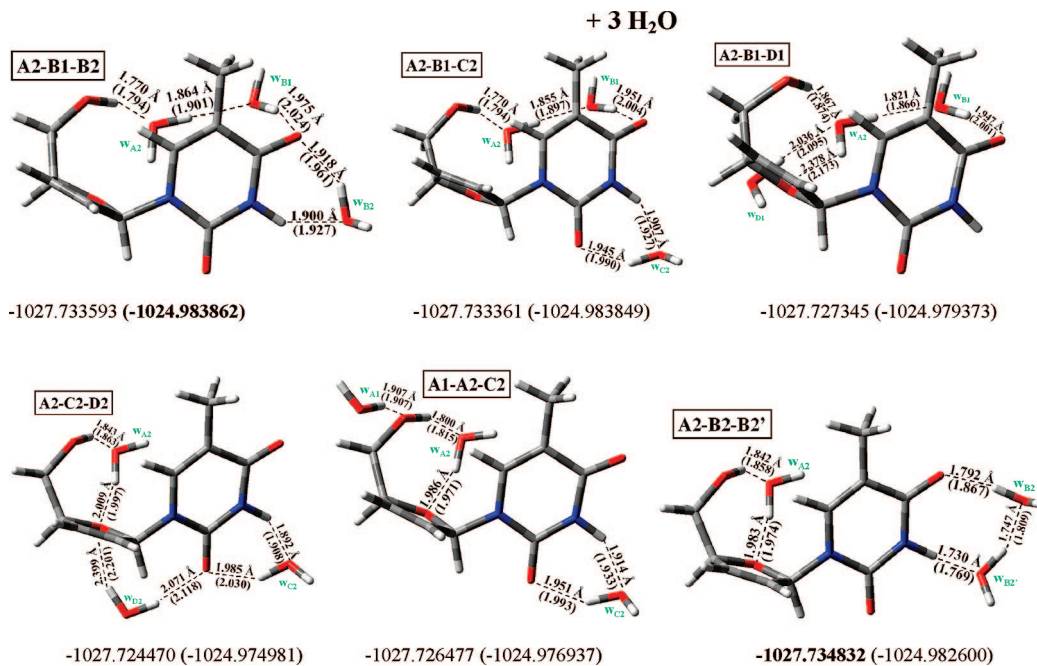


Figure 7. Optimum positions with three water molecules in the hydration of conformer I in D4T.

oxygens of the phosphate groups in nucleotides, to the ester oxygens of the phosphodiester linkages in polynucleotides, to the O4' oxygens of the furanose rings, and to the electronegative atoms of the base pairs.⁵⁶ In these studies it has been shown that the water molecule is a versatile connector that can serve as both hydrogen bond donor and acceptor. These water bridges contribute to the overall stability of helical conformers of DNA.⁵⁶

Several attempts have been made to decipher the effect of hydration on the photophysics of nucleic acid bases. Experimental efforts include mass spectroscopy and ionization potential measurements of gas-phase hydration complexes of thymine and adenine,⁵⁷ fragmentation pattern analysis of hydrated adenine and thymine,⁵⁸ UV spectroscopy of hydrated guanine formed in a supersonic jet,⁵⁹ and femtosecond pump–probe ionization mass spectroscopy of hydrated adenine clusters.⁶⁰ Theoretical

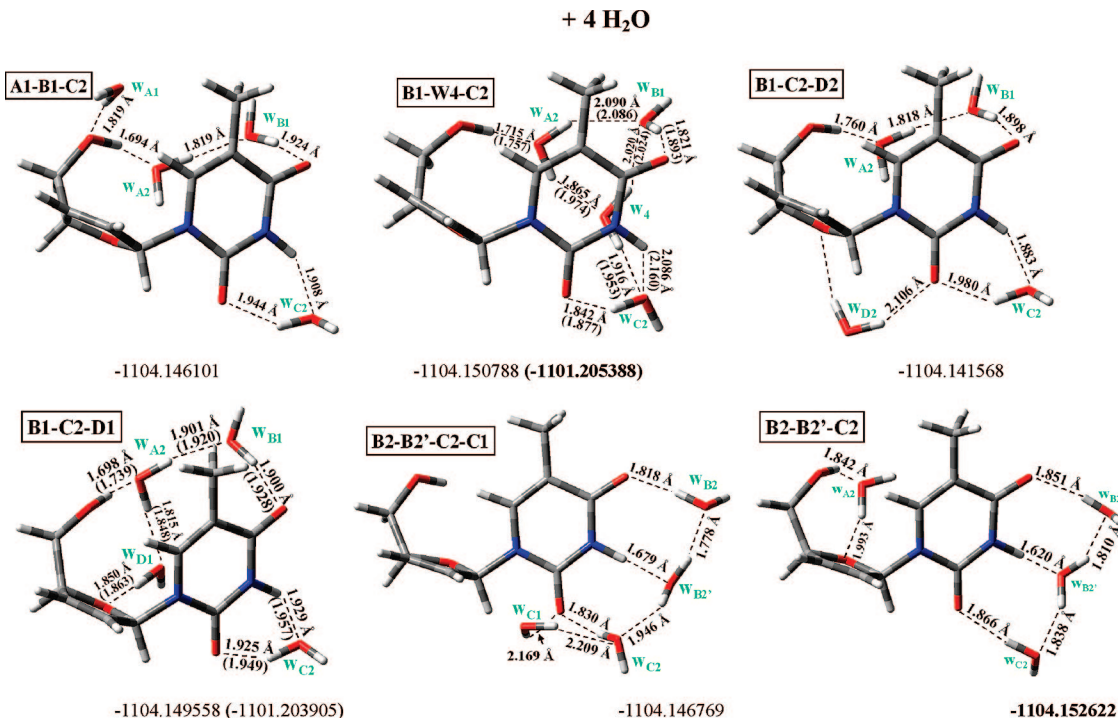


Figure 8. Optimum positions with four water molecules in the hydration of conformer I in D4T. For simplicity, the A2 water molecule was omitted from the notation of each cluster.

studies on the interaction between these bases with water molecules have also been performed.^{61,62} Despite these efforts, however, the effect of hydration on the geometrical parameters and vibrational spectra remains unclear. This understanding is crucial not only in terms of revealing the true origin of the activity of nucleic acid bases, but also in reconciling the differences between results from the gas phase and those from the condensed phase.⁵³

3.3.1. D4T Hydration. In the next sections, the methodology used with the successive addition of water molecules is shown. Thus, we determine the most stable clusters with water. We have seen that for D4T the first hydration shell is more-or-less complete with 13 water molecules. Moreover, experimentally,^{63,64} densimetric and ultrasonic measurements have been used to estimate the number of water molecules of hydration, which ranges between 12 and 20 per nucleotide pair. Also, the study reporting⁷⁰ on the hydration of guanine in the first solvation shell included 7–13 water molecules. Other experimental studies in methyl-substituted uracils and thymines reported that when more than four water molecules are attached, the photophysics properties of these hydrated clusters should rapidly approach that in the condensed phase.⁵³

Figures 3 and 6–10 show the order of filling of conformer I, and Figures 4 and 11 correspond to conformer II. Four regions in the D4T molecule, labeled as position A, B, C, and D, appear favorable for water molecules (Scheme 2). This notation is in accordance to that followed on the thymine molecule.⁵⁴ In these figures the water molecule is placed in all the possible stable positions, labeled as A1, A2, B1, B2, C1, C2, D1, and D2, where the number 1 or 2 refers to the number of intermolecular H-bonds of the water molecule. Water molecules are denoted as W_{A1} to W_{D2}, in reference to its position, when they can be clearly identified. In the other cases, such as W₁₀ to W₁₃, they are in reference to the number of water molecules added. For simplicity, weak H-bonds are not shown.

3.3.1.1. D4T-(H₂O)_n, n = 1–4. Monohydrated D4T-(H₂O). The first water molecule slightly changes the geometry and charge distribution. The main effect observed upon monohydration is the lengthening of the N–H and C=O bonds involved in the intermolecular H-bonds by 0.01 Å. By contrast, the neighboring N–C bonds (or N–C and C–C, cluster B2) shrank by 0.005 Å. This resembles in behavior of a typical amide bond in water (enhanced amide resonance due to solute–solvent interaction).⁶⁷ As expected, the C–H bonds are not sensitive to the presence of water, and the C_{methyl}–H bond has a very small lengthening, 0.0001 Å. Under hydration, the carbonyl oxygen and the amino nitrogen involved in the H-bonds show more negative charge, by 0.04 e[−] and 0.06 e[−], respectively, whereas the amino hydrogen is more positive, by 0.08 e[−].

The monohydrated clusters of conformer I are always more stable than those corresponding to conformer II, at the B3LYP and MP2 levels (Figures 3 and 4). The difference of energy between conformers I and II, 0.97 kcal in the isolated state at the B3LYP/6–31G** level, remains almost constant in the microhydrated D4T, although it is minimum in the **D1** cluster, 0.28 kcal/mol, and maximum in the **D2** cluster, 2.03 kcal/mol. The stability order of conformer I is:

A2	B2	C2	A1	D2	C1	B1
0 > 0.01 > 0.72 > 2.58 > 4.05 > 4.34 > 4.34 >						
0	1.92	2.42	3.19	4.69	6.14	6.54
					D1 5.48 (kcal by B3LYP)	
						6.77 (kcal by MP2)

The most stable cluster corresponds to A2 at both calculation levels. They are 0.01 kcal (1.92 by MP2) more stable than the next-most stable one, the **B2** cluster. These results indicate that the B3LYP method reproduces well the MP2 pattern of stability order. The relative energies by MP2 appear ca. 1.5 kcal higher than those by B3LYP.

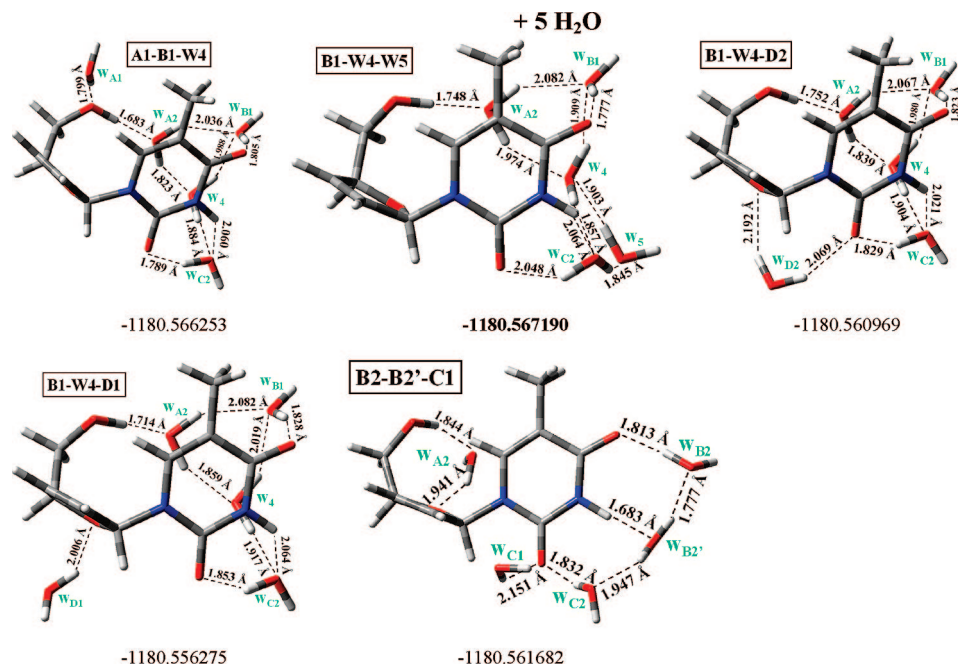


Figure 9. Optimum positions with five water molecules in the hydration of conformer I in D4T. For simplicity, the A2 and C2 water molecules were omitted from the notation of each cluster.

The water molecule in positions A2 and B2 represent the maximum CP-corrected complex formation energy ($E_{\text{D}4\text{T}W_1}^{\text{CP}}$) and interaction energy between D4T and the water molecule, $\Delta E_{\text{D}4\text{T}W_1}^{\text{CP}}$, Figure 5 and Table 6, and thus these positions are the most stable ones. In position A2, the D4T structure shows the maximum deformation energy of the D4T molecule, $E_{\text{D}4\text{T}}^{\text{def}}$, but very small in the water molecule, $E_{\text{W}_1}^{\text{def}}$. Position D1 of the water molecule has the minimum value of the interaction energy and, consequently, is less stable. The highest deformation energy of the water molecule appears in the B2 and C2 clusters due to the two H-bonds are strong and of similar strength, whereas in A2 the O^{4'}...H_w bond is slightly weaker. A similar trend was obtained by both calculation methods.

The monohydration of conformer II differs from that conformer I. The A2 and A1 forms are not stable by the low barrier height corresponding to the β torsional angle. In these cases, conformer II changes to conformer I (Figure 3). The two H-bonds of the water molecule in A2 of conformer I force the β torsional angle to the value of 88.7°, when in the isolated state it is 64.9° (Table 2), impeding the stability of conformer II with β angle of 164.4° in the isolated state. Therefore, the relation of stability in conformer II (Figure 4) is:

$$\text{B2} > \text{C2} > \text{B1} > \text{C1} > \text{D1} > \text{D2} \quad (\text{kcal by B3LYP})$$

$$0.90 > 4.14 > 4.40 > 4.96 > 5.27$$

The relative energy values appear close to those of conformer I. A comparison of these energies can be done with the results of Frigato et al.,⁵⁴ who performed MP2 ab initio calculations at high level for several thymine–water minima. Some similarity of the systems allows one to make a one-to-one correspondence between three of the minima structures reported and our data, appearing an accordance in the values. In uracil and thymine, region D, between the N1H and C2=O bonds, represents the region with a higher binding energy to water molecules.²⁷ However, in D4T this region appears impeded for binding to water molecules due to the presence of the furanose ring. The second-most stable region for binding to water molecules is the region B, between the N3H and C4=O bonds, in accordance to that found in the uracil molecule.²⁷

As in the uracil molecule,²⁷ the C2 cluster has the highest dipole moment. However, C1, D1, and A2 (the most stable) have the lowest values, decreasing the value of the isolated state; see Table 4. The mean error reported for the dipole moments⁷⁰ by MP2/6–31G** is 0.20 D, and that at the DFT level is 0.16 D, which does not significantly change the values.

With the hydration, a shift in the pseudorotation phase angle P is also observed (Tables 4 and 5). The D2 cluster brings about the greater change in the furanose ring conformation by both I and II conformers.

Geometry in the Monohydrated Clusters: Some selected optimized bond lengths and angles of monohydrated clusters at the B3LYP and MP2 levels are plotted in Figure 3. In the A2 cluster a water bridge is formed between the H5' atom of the OH group and the O4' atom of the furanose ring, stabilizing conformer I. A small lengthening of ca. 0.01 Å of the O5'–H and C4'–O4' bonds and an opening of ca. 1° of the C4'–C5'–O5' angle can be observed, while the rest of the structure remain almost constant. Values of distances and angles indicate a stronger H5'...O_w bond than O4'...H_w. In the furanose ring, the endocyclic ν_0 , ν_1 , and ν_3 and the exocyclic χ , β , and γ torsional angles are the most affected by the hydration.^{17,47} The remarkable change of the β angle up to 24° and in χ and γ angles of 7° and 2°, respectively, are noted (Tables 2 and 4). This is due to the water molecule being placed on the furanose ring, which forms two intermolecular H-bonds, one with O4' and another with the hydrogen of the –O5'H group. This produces a deformation of the D4T structure, the highest $E_{\text{D}4\text{T}}^{\text{def}}$ (Figure 5). There is no observed interaction of this water molecule with the H6 hydrogen of the thymine moiety (ca. 3 Å). The C5'–O5'–H5' and C4'–C5'–O5' angles remain almost unchanged (ca. 0.2° and 1.5°, respectively) with the hydration, indicating that this water molecule mainly produces a rotation of the O5'H group. The methyl group remains little affected by this water molecule. The strong H-bonds with water lead to a remarkable enhancement of the charges on O5', H5', and O4' atoms (Figure 2 for isolated state) and, therefore, to an increase of the reactivity. This increase of the reactivity is accompanied

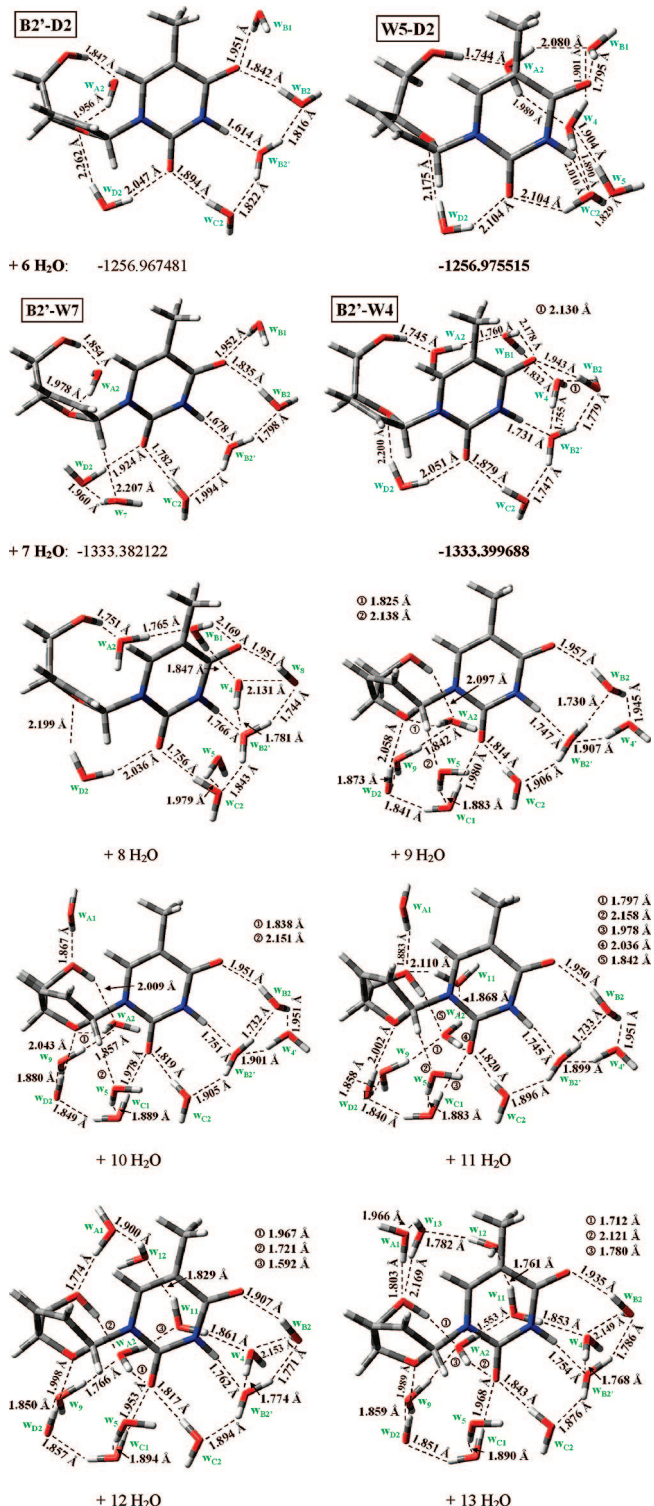


Figure 10. Optimum forms from 6 up to 13 water molecules in the simulation of the first hydration shell of conformer I in D4T.

by an increase in the energies of the HOMO and LUMO, with values of -0.349 and 0.100 , respectively, versus -0.342 and 0.103 , respectively, in an isolated state by MP2. Analyzing the effect of this water molecule in the weak intramolecular H-bonds, it can be noted that the weak H-bond between O₂ and H_{1'} remains almost unchanged. The H-bond between O_{4'} and H₆ does not appear in the monohydrated as well as in the isolated state. The weak H-bond between O_{5'} and H₆ remains. A notable reduction of the dipole moment, 3.95 D (4.98

D by MP2) with W_{A2} water molecule versus 4.89 D (5.91 D by MP2) in the isolated state, is also observed (Table 2).

In the **B2** and **C2** clusters the water molecule makes two simultaneous H-bonds to amino hydrogen and carbonyl oxygen of the thymine ring. The water hydrogen and oxygen atoms involved in the hydrogen bond are coplanar with the thymine moiety, whereas the second H is pointed out of the plane. The higher stability of B2 than C2 is due to the larger basicity of the O₂ atom than the O₄ atom.⁶⁵ Both clusters show similar behavior to monohydrated uracil,²⁷ with the water molecule slightly rotated and with C=O[•]...H_w—O_w angle of ca. $7\text{--}8^\circ$. Because of the presence of the methyl group, the **B1** cluster is somewhat different to those discussed above. Thus, the water molecule is positioned outside of the thymine plane, and one of the two strong H-bonds in B2 is substituted by a weak H_{8(methyl)}...O_w bond of 2.378 \AA (2.455 \AA by MP2), and with a C7—H₈...O_w value of 141.8° . This weak H-bond produces a small rotation of the methyl group, with a C4—C5—C7—H₁₀ torsional angle of 171.2° (174.3° by MP2). It has been postulated that C—H...O hydrogen bonds also contribute to the structural rigidity and stability of nucleic acids.^{50,55,66} Such H-bonds could be important in maintaining a helical conformation. The **A1**, **C1**, **D2**, and **D1** clusters appear because of the furanose moiety. In A1 the water molecule is H-bounded through a O_{5'}...H_w bond with a O_wH_w...O_{5'} angle of 165.7° (167.7° by MP2), and through a weak H₆...O_w bond of 2.303 \AA (2.316 \AA by MP2). The C6—H₆...O_w angle is 159.8° . The second H atom appears pointed out of the molecular structure. A notorious enhancement of the charges on O_{5'}, H_{5'}, and H₆ atoms, up to -0.829 , 0.509 , and 0.273 e^- , respectively, by MP2, is observed. In the **C1** cluster, the water molecule is also positioned outside of the thymine ring, with N1—C₂=O₂...H_w and C₂=O₂...H_w—O_w torsional angles of 2.1° and -43.3° , respectively, whereas the O_wH_w...O₂ angle is 156.6° . This fact is due to a weak H_{1'}...O_w bond of 2.303 \AA (2.328 \AA by MP2) and with a C1'—H1'...O_w angle of 174.2° (173.9° by MP2), which stabilize this cluster. The second H atom is pointed out of the molecular structure. A weak enhancement of the charges on C₂, O₂, and H_{1'} atoms, up to 1.042 , -0.780 , and 0.271 e^- , respectively, by MP2, is observed. In the **D2** cluster the water molecule is triply H-bounded weakly through H_w...O₂, H_w...O_{4'}, and H_{1'}...O_w of 2.416 \AA . The values of the angles are O_wH_w...O₂ of 149.4° , O_wH_w...O_{4'} of 143.7° , and C1'—H1'...O_w of 123.7° . This cluster structure is the only one in which the three atoms of the water molecule participate in H-bonds, although with weak strength. In **D1** the water molecule lies outside of the furanose and thymine ring, and it is bounded through H_w...O_{4'} with an angle O_wH_w...O_{4'} of 146.7° (144.5° by MP2). The water molecule also appears stabilized with a weak H-bond O_w...H_{4'} of 2.835 \AA (2.659 \AA by MP2) and with C4'—H4'...O_w of 97.9° . A weak enhancement of the charges on O_{4'} and H_{4'} atoms, -0.697 and 0.241 e^- , respectively, by MP2, is observed.

D4T-(H₂O)₂. A second water molecule was added in the most stable cluster calculated in the monohydration, cluster **A2**. Successively, the same methodology has been applied for incorporating the rest of water molecules. The resulting cluster combinations are shown in Figures 6–10 for conformer I. Conformation II follows a different trend in the addition of water molecules, as it is shown in Figure 11.

In some case, to asses that we really obtain the most stable cluster, other combinations were also optimized, including combinations with the water molecule in cyclic dimer form with linear H-bonds (Figure 6). In this last case, the B3LYP binding energy of these cluster structures were the highest ones, but it

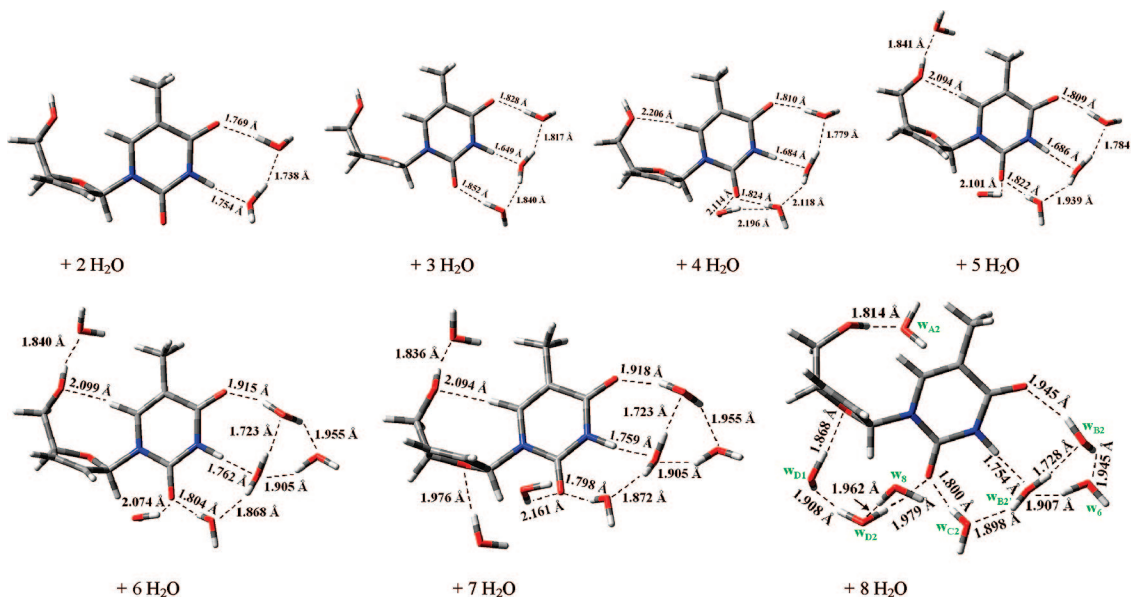


Figure 11. Optimum forms with two to eight water molecules in the simulation of the first hydration shell of conformer II in D4T. With eight water molecules, conformer II changes to conformer I.

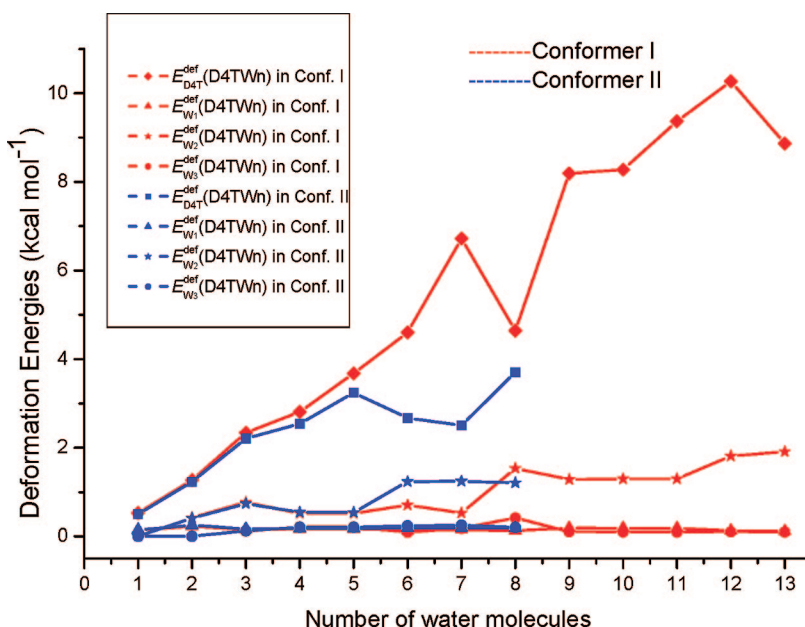


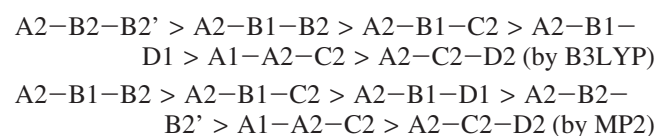
Figure 12. Deformation energies of D4T and the three first water molecules A2, B1, B2 (W1, W2, W3, respectively) into the complex.

is different by MP2. This difference is due to the intermolecular H-bond by B3LYP that is stronger between water molecules than between a water molecule and the nucleoside.

It is noted that the stability order of the different structures changes from B3LYP to MP2 calculations. It is well-known in literature that MP2 energies are much better than B3LYP energies, thus we have considered MP2 energies for determining the most stable cluster. For clusters with two water molecules, calculations at the MP2/6-31G** level confirm that the A2-B1 cluster is the most stable one (Figure 6).

In general, the bond lengths and angles obtained with the B3LYP method are close to those with the MP2 method. Figures 3 and 6-8 confirm the adequacy of the B3LYP method for the calculation of these parameters. However, it has been reported⁷⁰ that H-bonds are calculated by DFT methods somewhat too short, as a rule. Thus, the analysis of the H-bonds was carried out considering the MP2 values as more accurate.

D4T-(H₂O)₃. Following the same methodology as before, a third water molecule was added in the most stable dihydrated cluster calculated, A2-B1. The results obtained are shown in Figure 7. The stability order in conformer I is:



The main difference between B3LYP and MP2 appears as a consequence that the W_{B2}...W_{B2'} water dimer is more stable by B3LYP than the W_{A2}...W_{B1} dimer, which is the most stable by MP2. It can be noted that the higher stability of the A2-B1-B2 cluster vs A2-B1-C2 is due to the higher stability of the W_{B2} water than the W_{C2}, as observed in the monohydration of D4T. Except for this feature, B3LYP reproduces well the stability trend in the trihydration of D4T. Due to the better

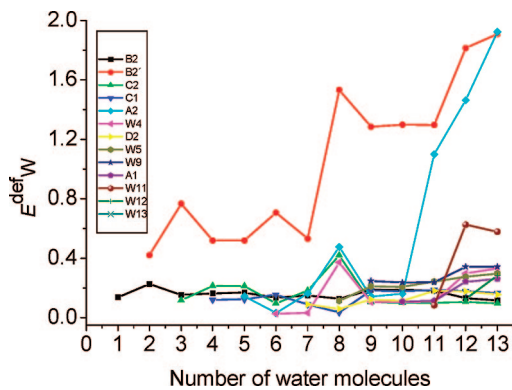


Figure 13. Deformation energies of each water molecule into the complex of D4T in conformer I.

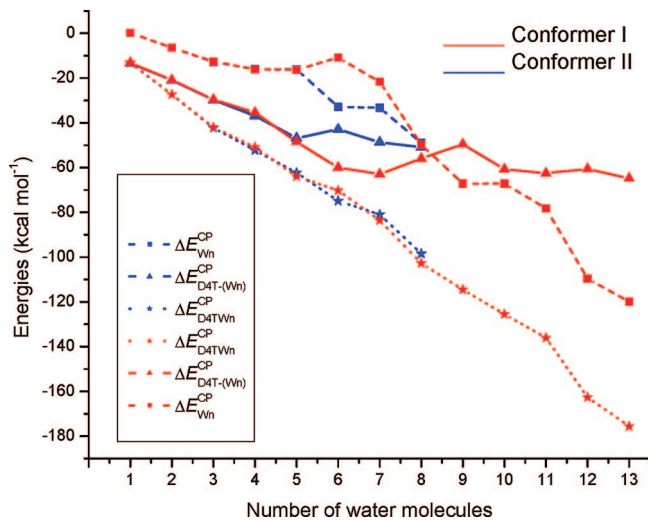


Figure 14. Complex formation and interaction energies for D4T-water and water-water.

energies calculated by MP2 than by B3LYP, the A2–B1–B2 cluster is considered as the most stable one.

$D4T-(H_2O)_4$. Following the same methodology by MP2, the addition of a fourth water molecule W_{C2} to the triple-hydrated cluster A2–B1–B2 leads to the tetrahydrated-cluster B1–W4–C2 as the most stable one. The results obtained are shown in Figure 8. For simplicity, in the notation used for each cluster the A2 water molecule is omitted. This addition produces a remarkable change in the W_{B2} water molecule (denoted as W_4) and leads to the establishment of a small water net. It is due to the preferred H-bond formation between water molecules than between a water molecule and D4T. This water net at one face of the D4T molecule leads the hydration direction. Because of the high computational demand, calculations at the MP2/6–31G* level were only performed for doubtful structures.

3.3.1.2. $D4T-(H_2O)_n$, $n = 5–12$. For cluster with 5–12 water molecules, MP2 calculations were not possible. The results with five water molecules appear plotted in Figure 9. For simplicity, the A2 and C2 water molecules are omitted in the notation used for the clusters. By B3LYP, the most stable structure corresponds to B1–W4–W5, with the W_5 water molecule H-bonded to W_4 and W_{C2} .

It is noted that, in general, there is a significant change in the χ and β torsional angles when the fourth and fifth water molecules are introduced; see Table 2. The lengthening of the C=O and N–H groups involved in intermolecular H-bonds is analogous to that observed in conformer II.

Two selected clusters structures with six water molecules appear plotted in Figure 10. For clarity, the A2, B1, B2 (or

W4), and C2 water molecules are omitted in the notation used for these clusters.

With seven water molecules a remarkable decrease, ca. 13°, of the χ torsional angle is observed (Table 2), leading to a different pseudorotation phase angle P and sugar conformation.

It is important to see in Figure 11 that when the eight water molecules are added, conformer II changes to conformer I, by rotation of the β torsional angle. Thus, conformer I is the only stable one with the further addition of water molecules. This is due to the preferred H-bonds among water molecules than between water and D4T. This cluster shows a drastic change in the deformation energies, Figures 12 and 13.

The cluster with nine water molecules shows a drastic change in the distribution of the water molecules. The further addition of water molecules increases the complexity of the hydration pattern, which is derived from an extraordinary variety of orientations displayed by the water molecules. The resulting orientation of these water molecules are represented by the complicated network of H-bonds as shown in Figure 10, being the W_{A2} water the central molecule, as well as W_{11} in the hydration with 12 and 13 water molecules.

3.3.1.3. $D4T-(H_2O)_{13}$: First Hydration Shell Effects. The first observed characteristic in the hydration with explicit water molecules is that all the water molecules appear H-bonded at the same face of the D4T molecule. It is due to two features: (i) the first water molecule added was in the A2 position, and it is the most stable one; and (ii) the H-bonds between water molecules are more stable than between a water molecule and the D4T molecule. Thus, the direction of hydration is marked for this first water molecule, and it can be observed with the successive hydration.

In the DNA hydration bibliography different names have been used for the several figures building with water molecules, such as “cone of hydration”,⁵⁵ or “pentagon of hydration”.⁵² Tentatively, these figures could be observed in Figure 10: the two water molecules only H-bonded on the O5' oxygen could be a “cone of hydration”, although very small; and the W_{A2} , W_{11} , W_4 , W_{B2} , and W_{C2} water molecules could be a “pentagon of hydration”, although irregular.

In general, the optimum distribution of the water molecules, binding to the most polar groups, is in accordance with the previous hydrated structure found in uracil molecule.²⁷

Another characteristic noted with the hydration is that the water molecules little affect the planarity of the pyrimidine ring, with change in its torsional angles of less than 2°. However, a lengthening of the C=O, N–H, and O–H bonds and an opening of the *ipso* ring angles involving in H-bonds are observed. Minor changes were observed for the χ and γ angles (ca. 3°). Comparing ours results with those of Arai et al.⁵⁵ suggests some regular orientation of water molecules in the first hydration shell.

In the intramolecular H-bonds the O2···H1' is 2.534 Å, remarkably longer than that in isolated state (2.224 Å), and the C1'–H1'···O2 angle is closer, 87.8°, than in the isolated state, 109.2°. These values indicate the breaking of the weak O2···H1' intramolecular H-bond observed in isolated state. It is due to the rotation of the thymine and furanose rings by effects of the 13 water molecules. As a consequence, the O4'···H6 and O5'···H6 distances appear far away with values of 3.553 and 3.344 Å, respectively, indicating the breaking of all the weak intramolecular H-bonds in the molecule.

The strong H-bonds with water lead to a general enhancement of the charges, especially on the oxygen atoms; see Figure 2. This fact increases the reactivity, and it is accompanied by an increase in the energies of the HOMO and LUMO, with values

of -0.259 and -0.058 , respectively, versus -0.238 and -0.038 in the isolated state.

Deformation Energies. In Figures 12 and 13 the calculated deformation energies appear plotted for D4T and water molecules as a consequence of the hydration with the successive addition of water molecules.

The deformation energies of each water molecule into the complex appear plotted in Figure 13. It can be noted that the water molecules $W_{B2'}$ and W_{A2} suffer the highest deformation, retaining the rest of the molecules with small changes. It can be explained as follows:

$W_{B2'}$ is the water molecule that remains most strongly H-bonded to the D4T. The $H_3 \cdots O_{WB2'}$ H-bond ranges from 1.614 (in the $B2'-D2$ cluster with six water molecules) to 1.766 Å in the cluster with eight water molecules. A jump in the energy appears with the addition of the eighth water molecule, due to a new H-bond of this $W_{B2'}$ water molecule with W_4 , although it produces a small lengthening ca. 0.01 Å of the $H_3 \cdots O_{WB2'}$ bond.

W_{A2} is the water molecule most H-bonded to other water molecules, such as W_{C2} , W_9 , and W_{11} . Moreover, the three atoms of the W_{A2} water molecule participate in strong H-bonds, one of them, the $H_{WA2} \cdots O_{W11}$ with the short value of 1.553 Å in the $D4T-(H_2O)_{13}$ cluster; see Figure 10. As consequence of this short H-bond, the W_{11} water molecule has a jump in the deformation energy to values of ca. 0.4 kcal/mol in the $D4T-(H_2O)_{12}$ and $D4T-(H_2O)_{13}$ clusters; see Figure 13.

Because of the high deformation observed in the $W_{B2'}$ water molecule, Figure 13, this molecule and the neighbors W_{B2} and W_{C2} bonded to $C4=O$ and $C2=O$ groups, respectively, were plotted in Figure 12. The deformation energies of these water molecules (labeled now as W_2 , W_1 , and W_3 , respectively) appear compared with those calculated in the D4T molecule. It can be noted that the deformation energy is much higher in D4T than in the water molecules. Also, it is noted that the conformer I of D4T appears more stabilized with the hydration than conformer II, and this stabilization increases with the successive addition of water molecules. In both conformers the $W_{B2'}$ water molecule appears with much higher deformation energies than the other two water molecules, and this energy also increases with the successive hydration. Figure 14 shows the calculated complex formation and interaction energies D4T-water, and water–water. Both conformers have similar values. The CP-corrected $D4T-(H_2O)_n$ formation energy for D4T molecules, $\Delta E_{D4T\cdot\cdot\cdot H_2O_n}^{CP}$, always has larger values than that corresponding to D4T–water and water–water. With the addition of more than eight water molecules, the interaction energies water–water have larger values than the D4T–water. This fact is due to the preferred water–water H-bonds than water–D4T. With the progress in the hydration, the water molecules appear stronger H-bonded among themselves and more weak with the D4T molecule.

3.3.1.4. PCM. The PCM self-consistent reaction-field was applied in order to investigate the effect of the water on the energy of solvation and on the structure of the nucleosides. Conformer I appears in Table 1 as a saddle point by the PCM model, whereas conformer II corresponds to a stable minimum. This fact has been also observed in the conformers I and II of thymidine molecules. However, following the methodology followed here with explicit water molecules, conformer II is not stable so it changes to conformer I. This is because, in the PCM model, the external polar cavity attracts the hydrogen of the OH group to a more open structure such as conformer II. However, this model fails when water molecules can be introduced in the holes inside of the molecule, such as W_{A2} in

the D4T, and thymidine molecules, where closer structures are favored, such as conformer I. Thus, we can conclude that conformer I in D4T is the only form present in the first hydration shell.

Analyzing the effect of the water molecule in the weak intramolecular H-bonds, it can be noted that the $O2 \cdots H1'$ is 2.260 Å, which is only ca. 0.04 Å longer than that of the isolated state. The $C1'-H1' \cdots O2$ is 107.6 , which is only 2° more close than that of isolated state, that is, the weak H-bond between $O2$ and $H1'$ remains almost unchanged.

The value of the intramolecular H-bond $O5' \cdots H6$ is 2.523 Å, and the $C6-H6 \cdots O5'$ angle is 130.0° , very close to 2.511 Å and 130.7° , respectively, calculated in the isolated state, so the weak H-bond between $O5'$ and $H6$ also remains almost unchanged.

It can be noted that the effect of the hydration on the geometry of D4T is smaller with the PCM method than with 13 explicit water molecules. On the atomic charges and the energies of the HOMO and LUMO, the effect is almost null, with values of -0.235 and -0.035 , respectively, which are very close to -0.238 and -0.038 in the isolated state. So we can conclude that the PCM method does not reproduce well the hydration pattern of D4T.

3.3.1.5. Charges. The NBO charges on the atoms using the PCM model and with 13 explicit water molecules are shown in Figure 2 at the B3LYP/6-31G** level. It can be noted with hydration the slight increase (between 0.04 – 0.08 e $^-$) in the negative charge on the $O5'$ atom, being the atom with the highest negative charge in the molecule as in the isolated state. Similar increase in the negative charge is observed on the $O2$ and $O4$ oxygen atoms, between 0.05 – 0.09 e $^-$ on $O2$ and between 0.03 – 0.07 e $^-$ on $O4$. The effect on $O4'$ is very small, only an increment of 0.05 e $^-$.

The positive charges are also enhanced on $H5'$, ca. 0.04 e $^+$, and on $H3$, between 0.02 – 0.04 e $^+$. Thus, the main effect observed with the hydration, by both continuum and discrete methods, is a general enhancement of the positive and negative charges on the atoms, that is, an increase of their reactivity. The effect is almost null on the atoms of the furanose ring.

3.3.2. Thymidine Hydration. **3.3.2.1. Geometries.** Table 7 shows the ZPEs of conformers I and II for the two molecules under study in the isolated state and hydrated form simulated by continuum and by 13 explicit water molecules models. Analogous to D4T, conformer II in Thy is the most stable one with the PCM model. Table 8 shows the changes observed for Thy in the pseudorotation phase angle P, the exocyclic and endocyclic torsional angles, and the maximum torsion angle, $\nu_{\text{máx}}$, which describes the maximum furanose out-of-plane pucker. Very slight variations on these angles with the PCM model can be observed in both conformers. However, with 13 explicit water molecules, conformer I shows very little endocyclic torsional angles that render the furanose ring nearly planar, as well as lower χ and δ angles. The β angle has a different behavior; it increases in conformer I, but it changes drastically in conformer II.

Figure 1 shows the geometric changes under hydration in conformer I. At a difference of D4T, the cluster of Thy with 13 explicit water molecules can be in conformer I or Ia, by transformation from conformer II (Figure 15). This new cluster with conformer Ia is stabilized by a water molecule, W_{12} , H-bonded to $H3'$ and $H5'$. As consequence of this water molecule, the β torsional angle is remarkably rotated from 176.2° (conformer II in isolated state) to -74.9° in Ia. A water dimer $W_{13} \cdots W_{A1}$ also contributes to the stabilization of this

TABLE 8: Geometrical Features: Torsional Angles (in degrees) in Conformers I and II (in Parentheses) of Thymidine (Thy) Optimized at the B3LYP/6-31G and MP2/6-31G* Levels**

parameters	Thy (isolated)	Thy (isolated) MP2	Thy + 13H ₂ O ^c	Thy (PCM)
Exocyclic Torsion Angles				
β (H5'-O5'-C5'-C4')	69.5 (176.2)	72.0	117.1 (-74.9)	69.6 (178.7)
γ (O5'-C5'-C4'-C3' or O5'-C5'-C4'-O4')	61.4 (51.3) -57.7 (-68.8)	60.2 -57.8	51.2 (35.8) -69.4 (-82.8)	61.4 (51.3) -57.6 (-68.8)
χ (O4'-C1'-N1-C2 or O4'-C1'-N1-C6)	-119.1 (-129.9) 56.4 (48.8)	-117.9 56.5	-88.4 (-131.6) 75.8 (35.3)	-119.1 (-126.4) 56.5 (51.4)
δ (C5'-C4'-C3'-O3')	130.3 (142.7)	137.6	116.9 (85.5)	130.5 (145.8)
Endocyclic Torsion Angles				
ν_0 (C4'-O4'-C1'-C2')	-34.0 (-19.7)	-34.4	-0.9 (-39.5)	-33.9 (-15.2)
ν_1 (O4'-C1'-C2'-C3')	37.9 (33.1)	41.4	-0.4 (18.2)	37.9 (31.1)
ν_2 (C1'-C2'-C3'-C4')	-27.6 (-33.2)	-32.4	1.5 (7.8)	-27.7 (-34.1)
ν_3 (C2'-C3'-C4'-O4')	8.7 (22.7)	13.2	-2.1 (-31.4)	8.8 (26.2)
ν_4 (C3'-C4'-O4'-C1')	15.8 (-2.0)	13.2	1.9 (44.4)	15.6 (-7.1)
P^a	-42.92 (-15.38)	-37.24	44.27 (79.81)	-42.68 (-7.06)
ν_{\max}^b	37.69 (34.43)	40.7	2.09 (44.07)	37.68 (34.36)
furanose pucker	² T (E)	² T	⁴ T (O ⁺ T ₄)	² T (E)

^a tgP = ((ν_4 + ν_1) - (ν_3 + ν_0))/(2 ν_2 (sin(36) + sin(72)). ^b ν_{\max} = (ν_2)/(cosP). ^c In this column the values in parentheses correspond to conformer Ia.

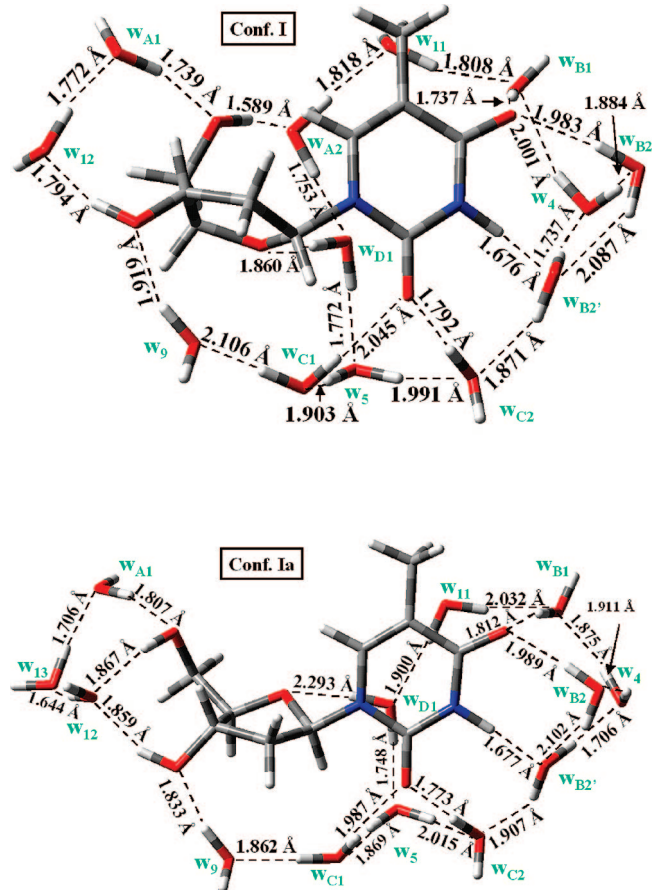


Figure 15. Optimum forms with 13 water molecules in the simulation of the first hydration shell of conformers I and II in Thymidine.

cluster Ia, leading to a more extended hydration shell than in conformer I.

In conformer I, as a consequence of the W₁₃...W_{A1} water dimer, the β torsional angle is remarkably rotated up to 117.1° (69.6° by PCM), whereas in the isolated state it is 69.5° (72.0° by MP2), and the O3'-H hydroxylic group appears remarkably rotated with ϵ (C2'-C3'-O3'-H3') torsional angle of 160.5°, whereas in the isolated state it is 69.8° (67.6° by MP2). Thus, according to the β and ϵ angle values in the discrete model for Thy in conformer I, the two hydroxyl groups O5'H and O3'H

are further apart. The PCM model does not reproduce this feature, and the ϵ angle, 69.7°, is similar to the isolated state.

A database of hydrated DNA X-ray structures shows that pyrimidines usually have a single associated water molecule, which can form a hydrogen bond to another base, often via a second water molecule (water bridges).^{55,69} Consistent with previous findings of Schneider et al.,⁶³ this water molecule can be found either in the major groove edge (region A, with O_w-H_w...O4) or in the minor groove edge (regions C and D, with O_w-H_w...O2), where it takes part in the so-called spine of hydration.⁶⁹ Because of their high mobility caused by the presence of large hydrophobic methyl groups, water molecules in the major groove were observed only in high-resolution, low-temperature B-DNA structures, whereas the minor groove base hydration is much more localized.^{63,69}

In B-DNA crystals, water molecules are also found in a position between region D and the methyl group.⁶³ In this structure, the water is weakly hydrogen bonded to the C-H of the methyl group and stabilized by the interaction with the phosphate group. Such interactions were found in our calculations. Moreover, hydration of DNA bases depends on the form of DNA, as it was demonstrated clearly for guanine in Z-DNA and in B-DNA.⁵² Generally, it is difficult for an X-ray crystallographic analysis to identify the H atoms, but recently, neutron diffraction experiments succeeded in determining most hydrogen atomic positions in the hydrated decameric d(CCATTAAATGG)₂ duplex.⁵⁵

3.3.2.2. Intramolecular H-Bonds. In conformer I of Thy with 13 explicit water molecules the O2...H1' H-bond is 2.262 Å (2.238 Å by PCM), which is only 0.02 Å longer than that of the isolated state, 2.238 Å. The C1'-H1'...O2 is 104.3° (108.4° by PCM), which is 4° closer than that of the isolated state, 108.4°, that is, this weak H-bond is further weakened with hydration.

The weak H-bond O5'...H6 in isolated state, 2.980 Å, shows a small strengthening under hydration, 2.584 Å (2.974 Å by PCM), and the C6-H6...O5' angle of 121.6° (149.1° by PCM), when in the isolated state, is 149.1°.

Analogously to D4T, Thy does not appear to have an intramolecular H-bond between O4' and H6. The value of O4'...H6 is 3.024 Å, and the C6-H6...O4' angle is 80.8°.

Conformer II of Thy with 13 explicit water molecules changes to conformer Ia. The O2...H1' remains almost unchanged,

TABLE 9: Intramolecular Distances of Interest among the Reactive Oxygen Atoms Calculated in the Molecules under Study

molecule	distance	B3LYP isolated	MP2 isolated	B3LYP PCM	B3LYP + 13 H2O
D4T	O5'...O2	5.921	5.820	5.889	4.616
	O5'...O4	6.426	6.254	6.423	6.292
	O5'...O4'	2.828	2.792	2.906	2.818
	O5'...O2	6.357	6.273	6.354	5.701
Thymidine	O5'...O4	7.372	7.255	7.365	6.178
	O5'...O4'	2.808	2.780	2.808	2.956
	O5'...O3'	4.357	4.344	4.359	4.194

2.264 Å, whereas the O5'...H6 disappears due to the value of 4.047 Å. By contrast, a weak H-bond O4'...H6 appears with 2.405 Å and C6—H6...O4' of 95.0°.

Finally, we noted that it has been reported⁶³ that the geometry of hydration around many bases in the DNA helix is very similar to that around the isolated bases.

3.3.2.3. Charges. Figure 2 shows the natural NBO atomic charges on the Thy atoms determined with the PCM model and with 13 explicit water molecules.

In both conformers of Thy, a water molecule appears H-bonded to O5' (Figure 10), leading as in D4T to a slight increase in the negative charge on O5' as compared to isolated state.

The O4 oxygen atom appears H-bonded to two water molecules in Thy, whereas in D4T to only one water molecule. Thus, its negative charge is higher in Thy (-0.707 e^-) than in D4T (-0.621 e^-). Analogous effects are observed in O2 and O4' atoms.

Comparison between the charges obtained in the isolated state and in the hydrated form shows the complexity of the polarizing effect of water on the Thy charge distribution. The more evident trends with the hydration are the enhancement of the negative charges on the oxygen and nitrogen atoms and the increase of the positive charge on the hydrogen bonded to nitrogen atoms. These features have also been observed in the hydration of thymine and cytosine.³⁹

3.3.2.4. Intramolecular Distances. Distances among the most reactive atoms, such as the oxygens, for isolated and hydrated forms in the two molecules under study appear collected in Table 9. The interest of these values is their relation with the possible acceptor sites in the enzyme, which will be the next step in our work.

Due to the almost planar furanose ring in D4T, its structure is closer than Thy with shorter (ca. 0.4 Å) O2...O5' and O4...O5' distances. The closeness of the O4' and O5' atoms leads to very small differences in the O4'...O5' distance between D4T and Thy. In isolated state the puckering of the furanose ring is higher in Thy than in D4T. This puckering in Thy brings nearer the O4' and O5' than in D4T with an almost planar ring.

In the hydration with 13 water molecules, the H-bonded water net with D4T is stronger than with Thy, with W_{A2} and W₁₁ as centrum; see Figure 10. This fact produces a closeness of the O5'-H5' group to the O2 atom through W_{A2} and leads to lower O2...O5', O4...O5', and O4'...O5' length values than in Thy.

4. Summary and Conclusions

In the present work we have studied the hydration of D4T and Thy and the influence of water on the stability of the different conformers. A good agreement is obtained, whenever available, with analogous theoretical studies, supporting the quality of our results derived from computations. The most important findings of the present work are the following:

(1) The different conformers of the D4T were accurately reproduced by MP2 and B3LYP. The values of the geometric parameters calculated were within the range of the mean absolute errors reported with these methods. The geometries and values of the properties presented here appear to be the most accurate to date.

(2) For understanding its structure, conformer, and possible behavior in physiological conditions of D4T and Thy, more than 200 cluster-optimized structures with water molecules have been obtained for the first time at the MP2 and B3LYP levels for the two most stable conformers. An observed feature in the hydration with explicit water molecules is that all the water molecules appear H-bonded at the same face of the nucleoside.

(3) In the isolated state, conformer I (anti-gg-gg) is the most stable for the D4T molecule. Conformer II appears stabilized by a weak intramolecular H-bond between the oxygen O5' and the hydrogen H6 of the thymine moiety, but in the hydration simulated with eight water molecules this conformer II is not stable, and the β torsional angle rotates to the value of conformer I. Thus, conformer I is the stable one with the further addition of water molecules in the simulation of the first hydration shell.

(4) By contrast, in the isolated state, conformer II (anti-gg-gt) for Thy is the most stable. This is due to weaker intramolecular H-bonds than in D4T. In hydrated form both conformers are stable, although in the hydration simulated with 12 water molecules conformer II ($\beta \approx 180^\circ$) is not stable, and the β torsional angle rotates to the value of conformer Ia ($\beta \approx -70^\circ$). As a consequence that the water molecules H-bonded between the two hydroxyl groups, the first hydration shell are more extended in both conformers of Thy than in D4T.

(5) We have located eight minima for the monohydration of D4T molecule. The water molecule offers the most stable structure in A2, B2, and C2 positions. A single water molecule in A2 strongly stabilizes conformer I versus conformer II, which is not stable.

(6) The interaction energy of the water molecule with only one intermolecular H-bond to the nucleoside is always lower than those with two H-bonds.

(7) The cluster structures with the water in dimer form are more stable than those with two single water molecules. The O...H intermolecular H-bond is stronger between water molecules than between a water molecule and the nucleoside.

(8) The standard methodology of adding water molecules to the most stable cluster obtained previously leads to very stable cluster structures, but not always to the global minimum. A check of similar cluster structures is necessary for this task, and it was carried out in the present work. MP2 calculations are necessary due to the deficiencies of B3LYP in some clusters.

(9) The optimum distribution of water molecules, binding to the most polar groups, are in accordance with the previous hydrated structure found in thymine and uracil molecules.

(10) The PCM model appears to fail in the molecules under study due to explicit water molecules can be introduced in the holes inside of the molecule stabilizing conformers that appears

as saddle point by PCM. Also, the PCM model remarkably underestimates the deformation of the structure by the water molecules.

(11) When the hydration is reproduced with only one or two water molecules, the use of a continuous solvent method gives a better geometry structure. However, when three or more molecules are used to reproduce the first hydration shell, the geometric values are better than those of the PCM model. With few water molecules the nucleoside structure is more deformed than with much more water molecules, because the intermolecular H-bonds are preferred among water molecules than between water molecules and the nucleoside.

(12) The variety of observed orientations of the water molecules causes the complexity of the hydrogen bond network shown. The complex formation energies are increased according to the increment of the number of water molecules, as well as the deformation energies of the nucleoside and in fewer amounts of each one water molecules.

Finally, we noted that it is possible to generalize the hydration simulation determined in these nucleosides to other relevant related ones.

Acknowledgment. The authors wish to thank the MCYT (Spain), project Nos. CTQ2006-14933/BQU and BQU2002-02875 for financial support, the Computational Center at Universidad Complutense of Madrid for running the Gaussian program package, and the Computational Chemistry Laboratory at Universidad Nacional de Educación a Distancia (Laboratory-QC, UNED).

References and Notes

- (1) Weiss, R. A. *Science* **1993**, *260*, 1273.
- (2) Kuipers, M. E.; Swart, P. J.; Hendriks, M.M.W.B.; Meijer, D. K. F. *J. Med. Chem.* **1995**, *38*, 883.
- (3) Furman, P. A.; Fyfe, J. A.; St. Clair, M. H.; Wenhold, K.; Rideout, J. L.; Mitsuya, H.; Barry, D. W. *Proc. Nat. Acad. Sci. USA* **1985**, *83*, 8333.
- (4) Sochacka, E.; Bawrot, B.; Pamkiewicz, K. W.; Watanabean, K. A. *J. Med. Chem.* **1990**, *33*, 1995.
- (5) Watanabe, K. A.; Harada, K.; Zeidler, J.; Matulic-Adamic, J.; Takahasi, R.; Ren, W.; Cheng, L.; Fox, J. J.; Chou, T.; Zhu, Q.; Polsky, B.; Gold, J. W. M.; Armstrong, D. J. *Med. Chem.* **1990**, *33*, 2145.
- (6) Ciuffo, G. M.; Santillan, M. B.; Estrada, M. R.; Yamin, L. J.; Jáuregui, E. A. *J. Mol. Struct. (Theochem)* **1998**, *428*, 155.
- (7) De Clercq, E. *J. Clin. Virol.* **2001**, *22*, 73.
- (8) De Clercq, E. *Biochim. Biophys. Acta* **2002**, *1587*, 258.
- (9) Newman, D. J.; Cragg, G. M.; Snader, K. M. *Nat. Prod. Rep.* **2000**, *17*, 215.
- (10) Food and Drug Administration (FDA); uri: <http://www.fda.gov/quia/pepfar.htm>.
- (11) Seaton, R. A.; Fox, R.; Bodasing, N.; Peters, S. E.; Gourlay, Y. *Aids* **2003**, *17*, 445.
- (12) Naeger, L. K.; Margot, N. A.; Miller, M. D. *Antimicrob. Agents CH* **2002**, *46*, 2179.
- (13) Rejnek, J.; Hanus, M.; Kabelák, M.; Ryjácek, F.; Hobza, P. *Phys. Chem. Chem. Phys.* **2005**, *7*, 2006.
- (14) Morsy, M. A.; Al-Somali, A. M.; Suwaiyan, A. *J. Phys. Chem. B* **1999**, *103*, 11205.
- (15) Yekeler, H. *J. Mol. Struct. (Theochem)* **2004**, *684*, 223.
- (16) Danilov, V. I.; Anisimov, V. M.; Kurita, N.; Hovorun, D. *Chem. Phys. Lett.* **2005**, *412*, 285.
- (17) Alcolea Palafox M.; De la Fuente M.; Iza N. in preparation.
- (18) Obika, S.; Andoh, J.; Sugimoto, T.; Miyashita, K.; Imanishi, T. *Tetrahedron Lett.* **1999**, *40*, 6465.
- (19) Nava-Salgado, V. O.; Martínez, R.; Arroyo, M. F. R.; Galicia, G. R. *J. Mol. Struct. (Theochem)* **2000**, *504*, 69.
- (20) (a) Fidanza, N. G.; Suvire, F. D.; Sosa, G. L.; Lobayan, R. M.; Enriz, R. D.; Peruchena, N. M. *J. Mol. Struct. (Theochem)* **2001**, *543*, 185. (b) Yurenko, Y. P.; Zhurakivsky, R. O.; Ghomi, M.; Samijlenko, S. P.; Hovorum, D. M. *J. Phys. Chem. B* **2007**, *111*, 9655. (c) Shishkin, O. V.; Gorb, L.; Leszczynski, J. *Int. J. Mol. Sci.* **2000**, *1*, 17.
- (21) (a) Hoffmann, M.; Rychlewski, J. *Rev. Mod. Quantum Chem.* **2002**, *2*, 1767. (b) Yurenko, Y. P.; Zhurakivsky, R. O.; Ghomi, M.; Samijlenko, S. P.; Hovorum, D. M. *J. Phys. Chem. B* **2007**, *111*, 6263. (c) Yurenko, Y. P.; Zhurakivsky, R. O.; Ghomi, M.; Samijlenko, S. P.; Hovorum, D. M. *J. Phys. Chem. B* **2008**, *112*, 1240. (d) Gaigeot, M.-P.; Ghomi, M. *J. Phys. Chem. B* **2001**, *105*, 5007.
- (22) Jensen, F.: *Introduction to Computational Chemistry*; John Wiley & Sons Ltd.: Chichester, England 2002, 189.
- (23) Alcolea Palafox, M.; Nielsen, O. F.; Lang, K.; Garg, P.; Rastogi, V. K. *Asian Chem. Letts.* **2004**, *8*, 81.
- (24) Alcolea Palafox, M.; Rastogi, V. K. *Spectrochim. Acta* **2002**, *58* A, 411.
- (25) Alcolea Palafox, M. *Recent Res. Devel. PhysChem.* **1998**, *2*, 213.
- (26) Alcolea Palafox, M. *Int. J. Quantum Chem.* **2000**, *77*, 661.
- (27) Alcolea Palafox, M.; Iza, N.; Gil, M. *J. Molec. Struct. (Theochem)* **2002**, *585*, 69.
- (28) Fernández-Quejo, M.; De la Fuente, M.; Navarro, R. *J. Mol. Struct.* **2005**, *744*–747, 749.
- (29) Frisch, M. J.; Trucks, G. W.; Schlegel, H. B.; Scuseria, G. E.; Robb, M. A.; Cheeseman, J. A.; Montgomery, J. A. Jr.; Vreven, T.; Kudin, K. N.; Burant, J. C.; Millam, J. M.; Iyengar, S. S.; Tomasi, J.; Barone, V.; Mennucci, B.; Cossi, M.; Scalmani, G.; Rega, N.; Petersson, G. A.; Nakatsuji, H.; Hada, M.; Ehara, M.; Toyota, K.; Fukuda, R.; Hasegawa, J.; Ishida, M.; Nakajima, T.; Honda, Y.; Kitao, O.; Nakai, H.; Klene, M.; Li, X.; Knox, J. E.; Hratchian, H. P.; Cross, J. B.; Adamo, C.; Jaramillo, J.; Gomperts, R.; Stratmann, R. E.; Yazyev, O.; Austin, A. J.; Cammi, R.; Pomelli, C.; Ochterski, J. W.; Ayala, P. Y.; Morokuma, K.; Voth, G. A.; Salvador, P.; Dannenberg, J. J.; Zakrzewski, V. G.; Dapprich, S.; Daniels, A. D.; Strain, M. C.; Farkas, O.; Malick, D. K.; Rabuck, A. D.; Raghavachari, K.; Foresman, J. B.; Ortiz, J. V.; Cui, Q.; Baboul, A. G.; Clifford, S.; Cioslowski, J.; Stefanov, B. B.; Liu, G.; Liashenko, A.; Piskorz, P.; Komaromi, I.; Martin, R. L.; Fox, D. J.; Keith, T.; Al-Laham, M. A.; Peng, C. Y.; Nanayakkara, A.; Challacombe, M.; Gill, P. M. W.; Johnson, B.; Chen, W.; Wong, M. W.; Gonzalez, C.; Pople, J. A. *Gaussian 03*, Rev. B.04; Gaussian, Inc.: Pittsburgh PA, 2003.
- (30) Tomasi, J.; Mennucci, B.; Cancès, E. *J. Mol. Struct. (Theochem)* **1999**, *464*, 211.
- (31) (a) Miertus, S.; Tomasi, J. *Chem. Phys.* **1982**, *65*, 239. (b) Cossi, M.; Barone, V.; Cammi, R.; Tomasi, J. *Chem. Phys. Lett.* **1996**, *255*, 327. (c) Cancès, M. T.; Mennucci, B.; Tomasi, J. *J. Chem. Phys.* **1997**, *107*, 3032. (d) Barone, V.; Cossi, M.; Tomasi, J. *J. Chem. Phys.* **1997**, *107*, 3210. (e) Cossi, M.; Barone, V.; Mennucci, B.; Tomasi, J. *Chem. Phys. Lett.* **1998**, *286*, 253. (f) Barone, V.; Cossi, M.; Tomasi, J. *J. Comput. Chem.* **1998**, *19*, 404. (g) Barone, V.; Cossi, M. *J. Phys. Chem. A* **1998**, *102*, 1995. (h) Mennucci, B.; Tomasi, J. *J. Chem. Phys.* **1997**, *106*, 5151.
- (32) (a) Mennucci, B.; Cancès, E.; Tomasi, J. *J. Phys. Chem. B* **1997**, *101*, 10506. (b) Tomasi, J.; Mennucci, B.; Cancès, E. *J. Mol. Struct. (Theochem)* **1999**, *464*, 211. (c) Cossi, M.; Barone, V.; Robb, M. A. *J. Chem. Phys.* **1999**, *111*, 5295. (d) Cammi, R.; Mennucci, B.; Tomasi, J. *J. Phys. Chem. A* **2000**, *104*, 5631. (e) Cossi, M.; Barone, V. *J. Chem. Phys.* **2000**, *112*, 2427. (f) Cossi, M.; Barone, V. *J. Chem. Phys.* **2001**, *115*, 4708. (g) Cossi, M.; Rega, N.; Scalmani, G.; Barone, V. *J. Chem. Phys.* **2001**, *114*, 5691. (h) Cossi, M.; Scalmani, G.; Rega, N.; Barone, V. *J. Chem. Phys.* **2002**, *117*, 43. (i) Cossi, M.; Rega, N.; Scalmani, G.; Barone, V. *J. Comput. Chem.* **2003**, *24*, 669.
- (33) Carpenter, J. E.; Weinhold, F. *J. Molec. Struct. (Theochem)* **1988**, *169*, 41.
- (34) Reed, A. E.; Curtiss, L. A.; Weinhold, F. *Chem. Rev.* **1988**, *88*, 899.
- (35) Aamouche, A.; Berthier, G.; Cadioli, B.; Gallinella, E.; Ghomi, M. *J. Mol. Struct. (Theochem)* **1998**, *426*, 307.
- (36) Williamns, R. W.; Lorey, A. H. *J. Comput. Chem.* **1991**, *12*, 861.
- (37) Tomasi, J.; Persico, M. *Chem. Rev.* **1994**, *94*, 2027.
- (38) Williams, R. W.; Cheh, J. L.; Lowrey, A. H.; Weif, A. F. *J. Phys. Chem.* **1995**, *99*, 5299.
- (39) Alemany, C. *Chem. Phys. Lett.* **1999**, *302*, 461.
- (40) Danilov, V. I.; Van Mourik, T.; Poltev, V. I. *Chem. Phys. Lett.* **2006**, *429*, 255.
- (41) Gulbis, J. M.; Mackay, M. F.; Holan, G.; Marcuccio, S. M. *Acta Crystallogr.* **1993**, *C49*, 1095.
- (42) (a) Dyer, I.; Low, J. N.; Tollin, P.; Wilson, H. R.; Howie, R. A. *Acta Crystallogr.* **1988**, *C44*, 767. (b) Roey, van, O.; Taylor, E. W.; Chu, C. K.; Schinazi, R. F. *J. Am. Chem. Soc.* **1993**, *115*, 5365.
- (43) Kovacs, T.; Parkanyi, L.; Pelczer, I.; Cervantes-Lee, F.; Pannell, K. H.; Torrence, P. F. *J. Med. Chem.* **1991**, *34*, 2595.
- (44) Harte, W. E.; Starret, J. E., Jr.; Martin, J. C. Jr.; Mansuri, M. M. *Biochem. Biophys. Res. Commun.* **1991**, *175* (1), 298.
- (45) Gurskaya, G. V.; Bochkarev, A. V.; Zhdanov, A. S.; Dyatkina, N. B.; Kraevskii, A. A. *Mol. Biol.* **1991**, *25* (2), 401.
- (46) Gurskaya, G. V.; Tsapkina, E. N. *Abstracts of the Twelfth European Crystallographic Meeting Moscow* **1989**, *2*, 380.
- (47) Saenger, W. In *Principles in Nucleic Acid Structure*; Springer Verlag: New York, 1984; p 88.
- (48) Rastogi, V. K.; Singh, C.; Jain, V.; Alcolea Palafox, M. *J. Raman Spectrosc.* **2000**, *31*, 1005.
- (49) Cramer, C. J., *Essentials of Computational Chemistry*; John Wiley & Sons: Chichester, England, 2002; pp 265–268.

- (50) (a) Yurenko, Y. P.; Zhurakivsky, R. O.; Samijlenko, S. P.; Ghomi, M.; Horovum, D. M. *Chem. Phys. Lett.* **2007**, *447*, 140, and references therein. (b) Desiraju, G. R.; Steiner, T. *The Weak Hydrogen Bond*; Oxford University Press: New York, 1999. (c) Panigrahi, S. K.; Desiraju, G. R. *J. Biosci.* **2007**, *32* (4), 677.
- (51) Kubinec, M. G.; Wemmer, D. E. *J. Am. Chem. Soc.* **1992**, *114*, 8739.
- (52) Schneider, B.; Cohen, D. M.; Schleifer, L.; Srinivasan, A. R.; Olson, W. K.; Berman, H. M. *Biophys. J.* **1993**, *65*, 2291.
- (53) He, Y.; Wu, C.; Kong, W. *J. Phys. Chem. A* **2004**, *108*, 943.
- (54) Frigato, T.; Svozil, D.; Jungwirth, P. *J. Phys. Chem. A* **2006**, *110*, 2916.
- (55) Arai, S.; Chatake, T.; Ohhara, T.; Kuruhara, K.; Tanaka, I.; Suzuki, N.; Fujimoto, Z.; Mizuno, H.; Niimura, N. *Nucleic Acids Res.* **2005**, *33*, 3017.
- (56) (a) Vovelle, F.; Goodfellow, J. M., In *Hydration Sites and Hydration Bridges around DNA Helice*; Westhof, E., Ed.; Water and Biological Macromolecules, Topics in Molecular and Structural Biology; The Macmillan Press: London, 1993; *Vol. 17*, p 244. (b) Westhof, E., *Structural Water Bridges in Nucleic Acids*; Westhof, E. Ed.; Water and Biological Macromolecules, Topics in Molecular and Structural Biology; The Macmillan Press: London, 1993; *Vol 17*, p 226.
- (57) Kim, S. K.; Lee, W.; Herschbach, D. R. *J. Phys. Chem.* **1996**, *100*, 7933.
- (58) Kim, N. J.; Kim, Y. S.; Jeong, G.; Ahn, T. K.; Kim, S. K. *Int. J. Mass Spectrom.* **2002**, *219*, 11.
- (59) Piuzzi, F.; Mons, M.; Dimicoli, I.; Tardivel, B.; Zhao, Q. *Chem. Phys.* **2001**, *270*, 205.
- (60) Kang, H.; Lee, K. T.; Kim, S. K. *Chem. Phys. Lett.* **2002**, *359*, 213.
- (61) Marian, C. M.; Schneider, F.; Kleinschmidt, M.; Tatchen, J. *Eur. Phys. D* **2002**, *20*, 357.
- (62) (a) Sobolewski, A. L.; Domcke, W.; Dedonder-Lardeux, C.; Jouvet, C. *Phys. Chem. Chem. Phys.* **2002**, *4*, 1093. (b) Mourik, van, T.; Danilov, V. I.; Gonzalez, E.; Deriabina, A.; Poltev, V. I *Chem. Phys. Lett.* **2007**, *445*, 303. (c) Danilov, V. I.; Mourik, van, T.; Poltev, V. I *Chem. Phys. Lett.* **2006**, *429*, 255.
- (63) Schneider, B.; Berman, H. M. *Biophys. J.* **1995**, *69*, 2661.
- (64) Chalikian, T. V.; Sarvazyan, A. P.; Plum, G. E.; Breslauer, K. J. *Biochemistry* **1994**, *33*, 2394.
- (65) Chandra, A. K.; Uchimaru, T.; Zeegers-Huyskens, T. *J. Mol. Struct.* **2002**, *605*, 213.
- (66) Auffinger, P.; Louise-May, S.; Westhof, E. *Faraday Discuss.* **1996**, *103*, 151.
- (67) Blicharska, B.; Kupka, T. *J. Mol. Struct.* **2002**, *613*, 153.
- (68) Auffinger, P.; Westhof, E. *J. Mol. Biol.* **2000**, *300*, 1113.
- (69) Neidle, S. In *Nucleic Acid Structure and Recognition*; Oxford University Press: Oxford, UK, 2002.
- (70) Shukla, M. K.; Leszczynski, J. *J. Phys. Chem. B* **2008**, *112* (16), 5139.

JP806684V